REFERENCES

1. Dugave, C.; Demange, L. Cis-trans isomerization of organic molecules and biomolecules. *Chem. Rev.* 103 (2003): 2475-2532.
2. Saltiel, J.; Sun, Y.-P. *Photochromism, molecules and systems.* Edited by Durr, H.; Boaus-Laurent, H. Amsterdam: Elsevier , 1990.
3. Sumitani, M.; Nakashima, N.; Yoshihara, K., Direct measurement of the reaction rate for cis-trans photoisomerization of stilbene. *Chem. Phys. Lett.* 68 (1979): 255-257.
4. Waldeck, D. H. Photoisomerization dynamics of stilbenes. *Chem. Rev.* 91 (1991): 415-436.
5. Robert, J.-C.; Pincock, J. A. Methoxy-substituted stilbenes, styrenens and 1-arylpropenes: Photophysical properties and photoaddition of alcohols. *J. Org. Chem.* 71 (2006): 1480-1492.
6. Oriol, L.; Pinol, M.; Serrano, J. L.; Tejedor, R. M. Synthesis, Characterization and photoreactivity of liquid crystalline cinnamates, *J. Photochem. Photobiol. A* 155, (2003) 37-45.
7. Taylor, C. R.; Stern, R. S.; Leyden, J. J.; Gilchrest, B. A. Photoaging/photodamage and photoprotection. *J. Am. Acad. Dermatol.* 22 (1990): 1-15.
8. Taylor, C. R.; Sober A. J. Sun exposure and skin disease. *Annu. Rev. Med.* 47 (1996): 181-191.
9. Finlay, J. J.; Hart, P. H. Gamma(c) and the control by IL-4 of human macrophage proinflammatory mediator production. *Mut. Res.* 422 (1998): 155-159.
10. Ziegler, A.; Leffell, D. J.; Kunala, S.; Sharma, H. W.; Gailani, M.; Simon, J. A.; Halperin, A. J.; Baden, H. P.; Shapiro, P. E.; Bale, A. E. Mutation hotspots due to sunlight in the p53 gene of nonmelanoma skin cancers. *Proc. Nat. Acad. Sci. USA* 90 (1993): 4216-4220.

11. Mouret, S.; Baudouin, C.; Charveron, M.; Favier, A.; Cadet, J.; Douki, T. Cyclobutane pyrimidine dimers are predominant DNA lesions in whole human skin exposed to UVA radiation. *Proc. Nat. Acad. Sci. USA* 103 (2006):13765-13770.

12. Poon, T. S.; Barnetson, R. S.; Halliday, G. M. Sunlight-induced immunosuppression in humans is initially because of UVB, then UVA, followed by interactive effects. *J. Invest. Dermatol.* 125 (2005): 840-846.

13. Watanabe, H.; Shimizu, T.; Nishihira, J.; Abe, R.; Nakayama, T.; Taniguchi, M.; Sabe, H.; Ishibashi, T.; Sayre, R. M.; Dowdy, J. C. Photostability testing of Avobenzone. *Cosmet. Toil.* 114 (1999): 85-91.

14. Agar, N.S.; Halliday, G.M.; Barnetson, R.S.; Ananthaswamy, H. N.; Wheeler, M.; Jones, A. M. The basal layer in human squamous tumors harbors more UVA than UVB fingerprint mutations: a role for UVA in human skin carcinogenesis. *Proc. Nat. Acad. Sci. USA* 101 (2004): 4954-4959.

15. Jiang, R.; Roberts, M. S.; Collins, D. M.; Benson, H. A. E. Absorption of sunscreens across human skin: an evaluation of commercial products for children and adults. *Brit. J. Clin. Pharmaco.* 48 (1999): 635-637.

16. Pattanaargson, S; Limphong, P. "Stability of Octyl Methoxycinnamate and Identification of Its Photo-Degradation Product." *Int. J. Cosmet. Sci.* 23 (2001): 151-158.

17. Pattanaargson, S.; Munhapol, T.; Hirunsupachot, P.; Luangthongaram, P. "Photoisomerization of Octyl Methoxycinnamate" *J. Photochem. Photobiol. A* 161 (2004): 269-274.

18. Wahlberg, T.; Stenhagen, N.; Larko, G.; Rosen, O.; Wennberg, A.; Wennerström, O. Changes in ultraviolet absorption of sunscreens after ultraviolet irradiation. *J. Invest. Dermatol.* 113 (1999): 547-553.

19. Fourtanier, A.; Labat-Robert, J.; Kern, P.; Berrebi, C.; Gracia, A. M.; Boyer, B. In vivo evaluation of photoprotection against chronic ultraviolet-A irradiation by a new sunscreen Mexoryl SX. *Photochem. Photobiol.* 55 (1992): 549-560.

20. Ashby, J.; Tinwell, H.; Plautz, J.; Twomey, K.; Lefevre, P. A. Lack of binding to isolated estrogen or androgen receptors, and inactivity in the immature rat uterotrophic assay, of the ultraviolet sunscreen filters Tinosorb M-active and Tinosorb S. *Regul. Toxicol. Pharmacol.* 34 (2001): 287-291.

21. Luther, H.; Stehlein, A.; Minklei, M. (1996) International Patent Classification A61K 7/42, International Publication number WO 97/03643.

22. Thitinun Monhaphol, *Synthesis of cinnamate derivatives and related compounds as novel UV filters.* Master's Thesis, Graduate School, Chulalongkorn University, 2002.

23. Cantrell, A.; McGarvey, D. J.; Mulroy L.; Truscott G. T. Laser Flash Photolysis Studies of the UVA Sunscreen Mexoryl® SX *Photochem. Photobiol.,* 70 (1999): 292–297.

24. Kerry B. L.; Hanson M.; Simon J. D. Primary processes of the electronic excited state of *trans*-urocanic acid. *J. Phys. Chem. A* 101 (1997): 969-972.

25. Beeby, A.; Jones, A.E.; The Photophysical Properties of Menthyl Anthranilate: A UV-A Sunscreen, *Photochem. Photobiol.,* 72 (2000): 10-15.

26. Shindo, Y. Photoisomerization of ethyl cinnamate in dilute solutions, *J. Photochem.* 26 (1984), 185-192.

27. Ishigami, T.; Nakazato, K.; Uehara, M. Endo, T. Marked dependence of multiplicity in direct Z, E photoisomerization of a series of methyl cinnamates on their para-substituents, *Tett. Lett.* 10 (1979): 863-866.

28. Lewis, F. D.; Quillen, S. L.; Elbert J. E. The singlet states of methyl cinnamate and methyl indenoate, *J. Photochem. Photobiol., A* 47 (1989), 173-179.

29. Morliere, P.; Avice, O.; Sa E.; Melo, T.; Dubertret, L.; Giraud, M.; Santus, R. A Study of the Photochemical properties of some cinnamate sunscreens by steady state and laser flash photolysis. *Photochem. Photobiol.* 36 (1982): 395-399.

30. Gonzenbach, H.; Hill, T. J.; Truscott, T. G.; The triplet energy levels of UVA and UVB sunscreens, *J. Photochem. Photobiol. B* 16 (1992): 377-379.

31. Smith, G. J.; Miller, I. J. The effect of molecular environment on the photochemistry of *p*-methoxycinnamic acid and its esters, *J. Photochem. Photobiol. A*, 118 (1998): 93-97.

32. Lustres, J. L. P.; Farztdinov, V. M.; Kovalenko, S. A. Femtosecond S3→S1 conversion and structural reorganisation of trans-3-phenylprop-2-enaldehyde and derivatives in solution, *Chem. Phys. Chem.* 6 (2005): 1590-1599.

33. Lakowicz, J. R., *Principle of Fluorescence Spectroscopy*. New York: Kluwer Academic/ Plenum Publishers, 1999.

34. Monhaphol, T.; Albinsson, B.; Pattanaargson, S. 2-Ethylhexyl-2,4,5-trimethoxycinnamate and di-(2-ethylhexyl)-2,4,5-trimethoxybenzalmalonate as novel broadband UV filters *J. Pharm. Pharmacol.* 59 (2007): 279-288.

35. O'Conner, D. V.; Phillips, D. *Time-correlated single photon counting*. London Academic Press Inc., 1984.

36. Skoog, A. D.; West, D. M.; Holler, F. J. *Fundamentals of Analytical Chemistry*, 7th edited. USA: Saunders College Publishing, 1997.

37. Koo, J.; Fish, M. S.; Walker, G. N.; Blake, J. 2,3-Dimethoxycinnamic Acid" *Org. Syn. Coll.* vol 4 (1944): 327-328.

38. Womack, E. B.; McWhirter, J. Phenyl cinnamate *Org. Syn. Coll.* vol 3 (1943): 714-715.

39. Murov, S. L.; Cannichael, I; Hug, G. L. *Handbook of Photochemistry*. 2nd edited New York: Marcel Dekker, Inc., 1993.

40. Devanathan, S; Ramamurthy, V. Consequences of hydrophobic association in photoreactions: Photodimerization of alkyl cinnamates in water. *J. Photochem. Photobiol.* 40 (1987): 67-77.

41. Pavia, D. L.; Lampman, G. M.; Kriz, G. S. *Introduction to Spectroscopy*, USA: Thomson Learning, Inc., 2001.

42. Lippert, E. Z. Dipole moment and electronic structure of excited molecules. *Naturforsch* 10a (1955): 541-545.

43. Stickler, S. J.; Berg, R. A. Relationship between Absorption Intensity and Fluorescence Lifetime of Molecules *J. Chem. Phys.* 37(1962), 814-822.

44. Lewis, F. D.; Kalgutkar, R. S. The Photochemistry of *cis*-ortho-, meta-, and para-aministilbenes, *J. Phys. Chem. A* 105 (2001): 285-291.

45. Schieffer, S.; Pescatore, J.; Ulsh, R.; Liu, R. S. H. Regioselective Hula-twist photoisomerization of cinnamate esters in organic glass, *Chem. Commun.* (2004): 2680-2681.

46. Carey, F. A.; Sundberg, R. J. *Advanced Organic Chemistry*. 3rd edited, New York: Plenum Press , 1993.

47. Lewis, F. D.; Kalgutkar, R. S.; Yang, J. S. The Photochemistry of *trans-ortho-*, *meta-*, and *para*-aminostilbenes *J. Am. Chem. Soc.* 121 (1999): 12045-12053.

48. Roberts, J. C.; Pincock, J. Methoxy-substituted stilbenes, styrenes, and 1-arylpropenes: Photophysical properties and photoadditions of alcohols. *J. Org. Chem.* 71 (2006): 1480-1492.

49. Okereke, C. S.; Barat, S. A.; Abdel-Rahman, M. S. Safety evaluation of benzophenone-3 after dermal administration in rats. *Toxicol. Lett.* 80 (1995): 61-67.

APPENDICES

APPENDIX A

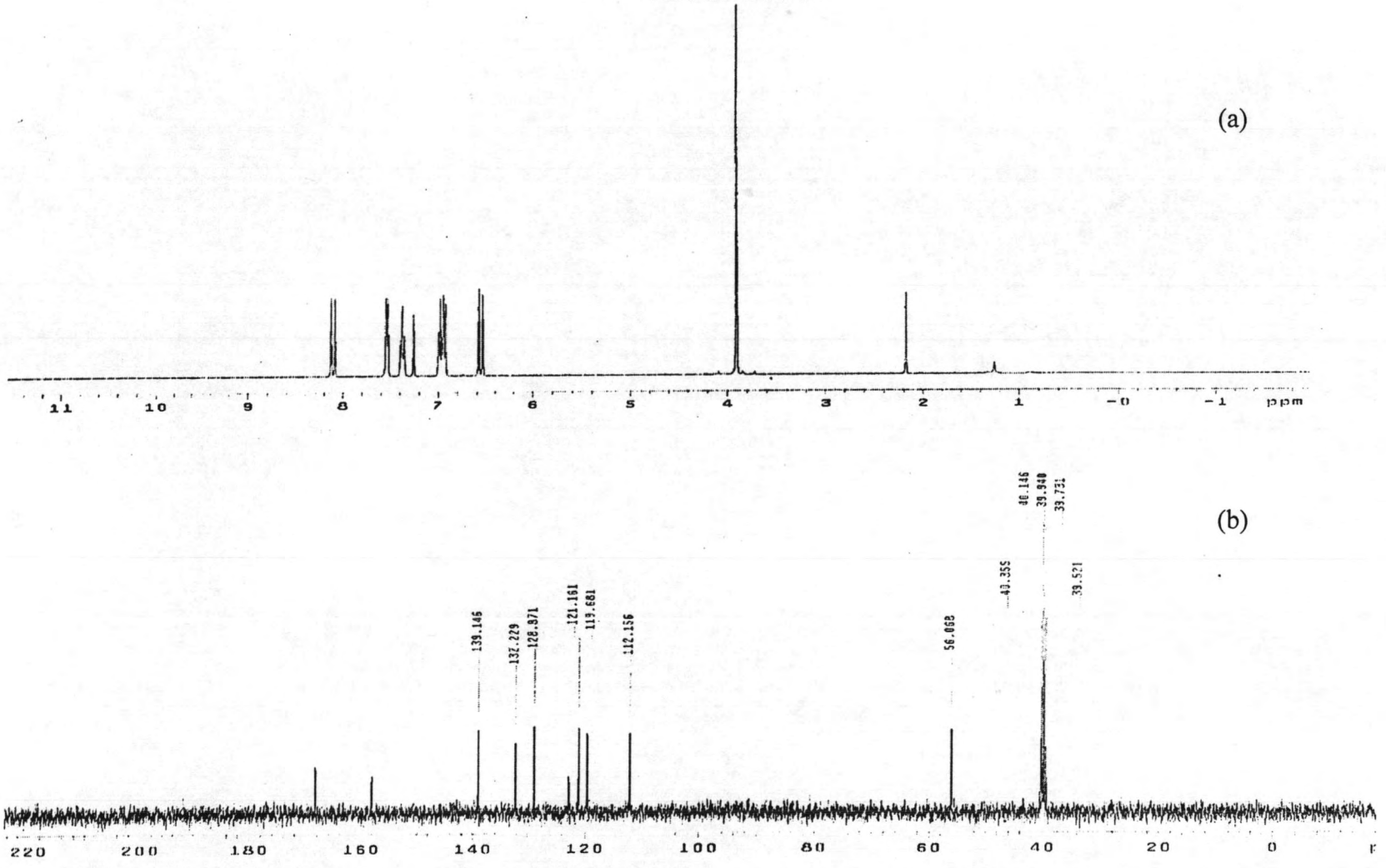

Figure A1 ^{1}H (a) and ^{13}C NMR spectrum (b) of 2-methoxycinnamic acid (**1A**) in DMSO-d_6

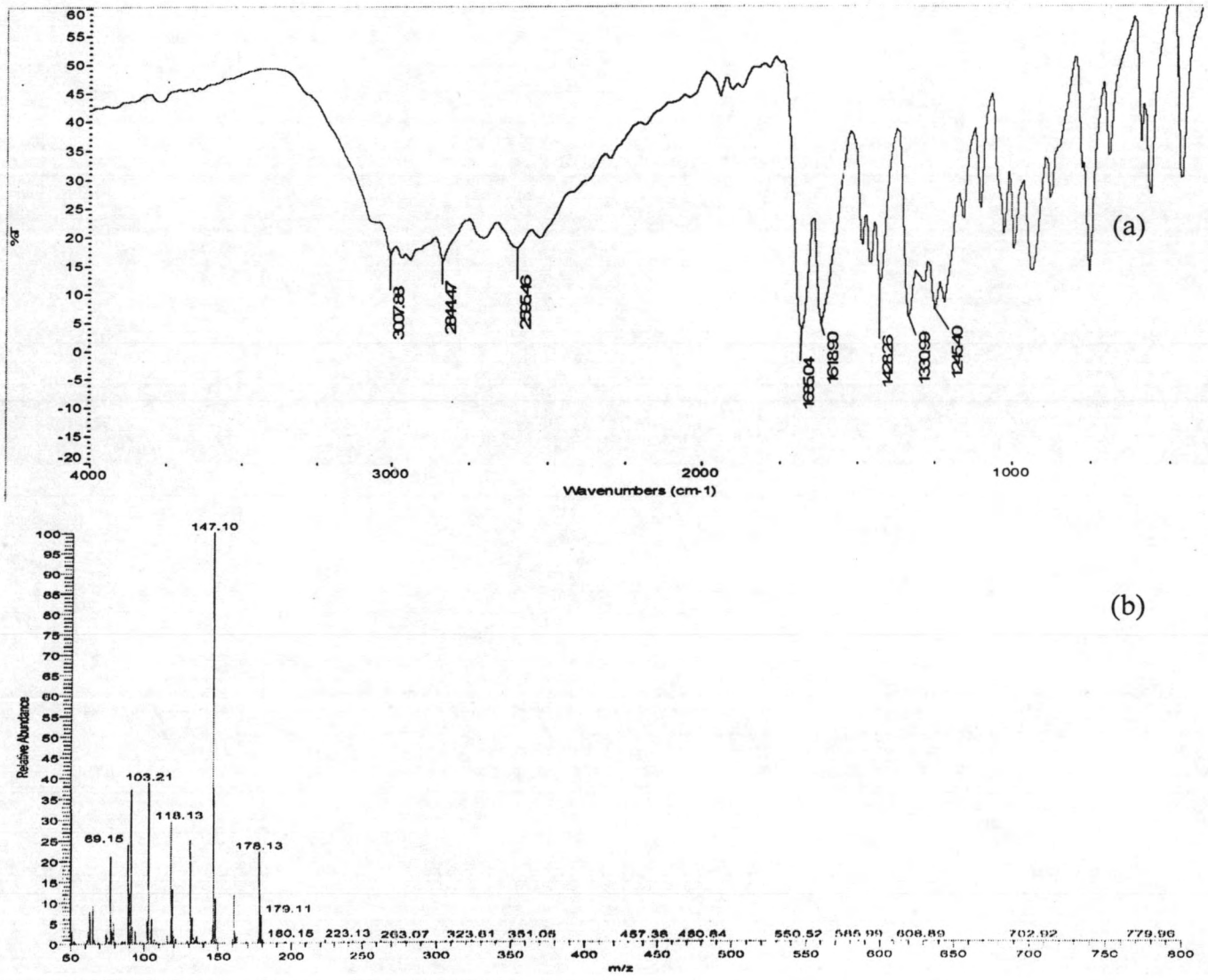

Figure A2 IR (a) and MS (b) spectrum of 2-methoxycinnamic acid **(1A)**.

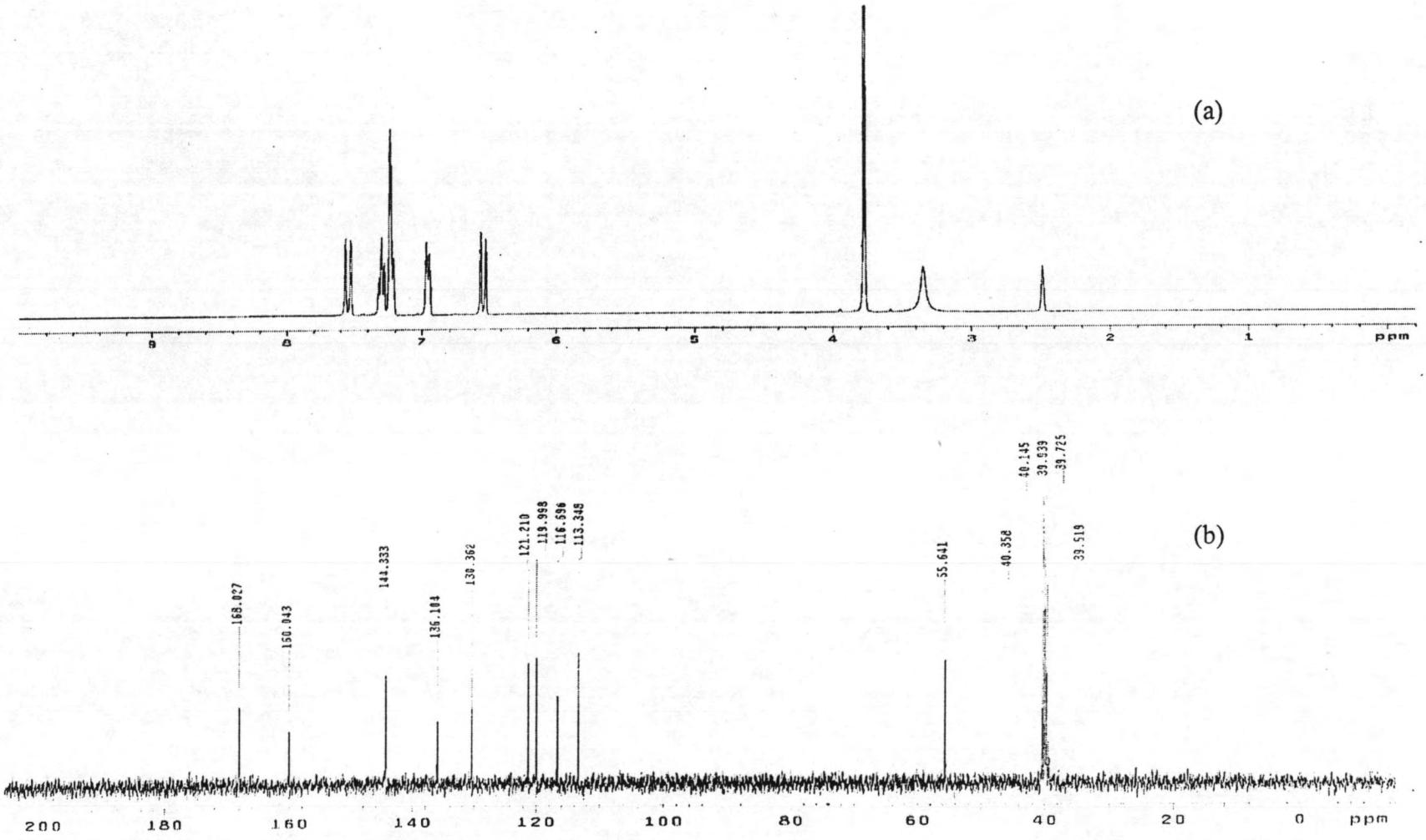

Figure A3 ^{1}H (a) and ^{13}C NMR spectrum (b) of 3-methoxycinnamic acid (**2A**) in DMSO-d_6

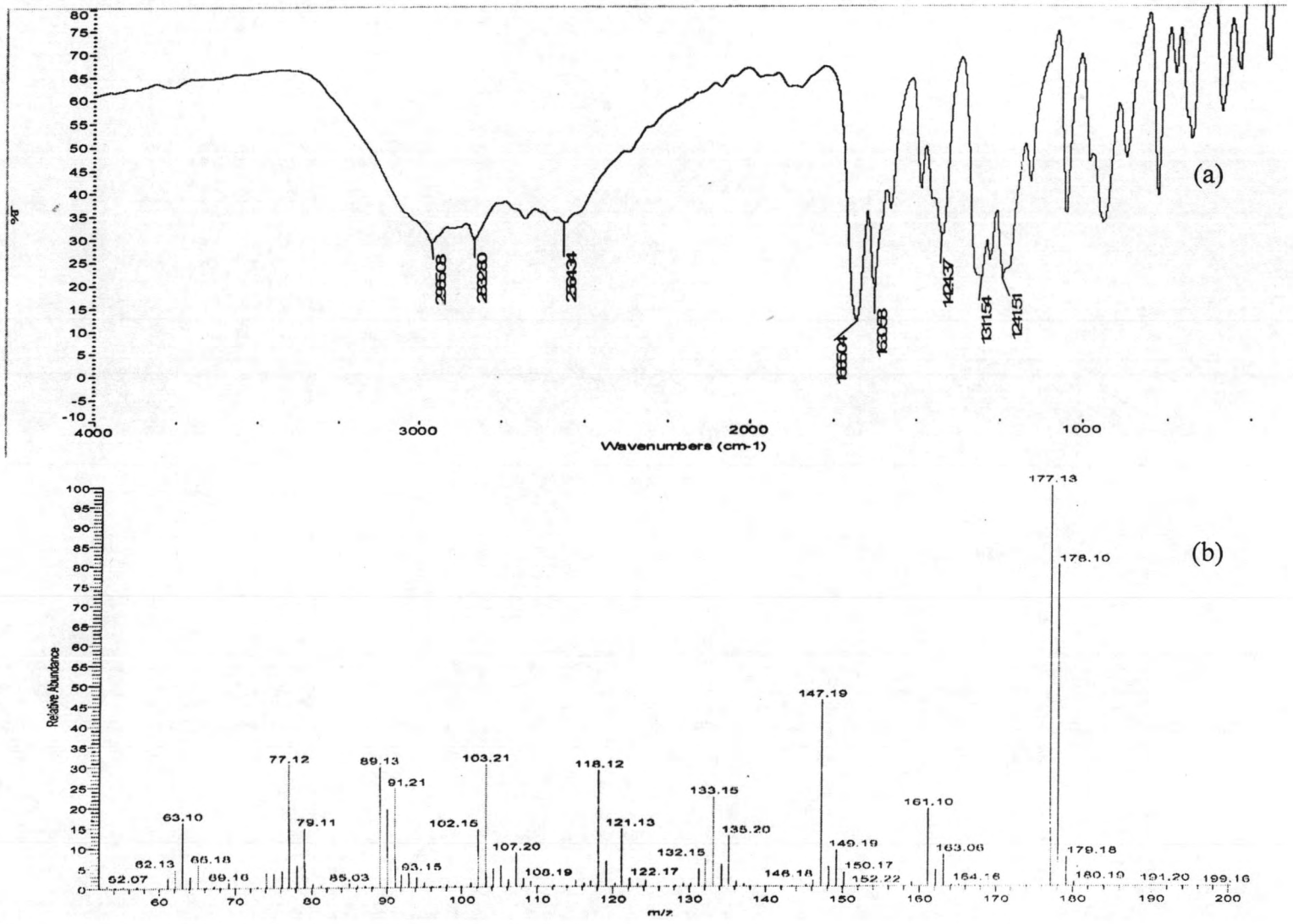

Figure A4 IR (a) and MS spectrum (b) of 3-methoxycinnamic acid (**2A**).

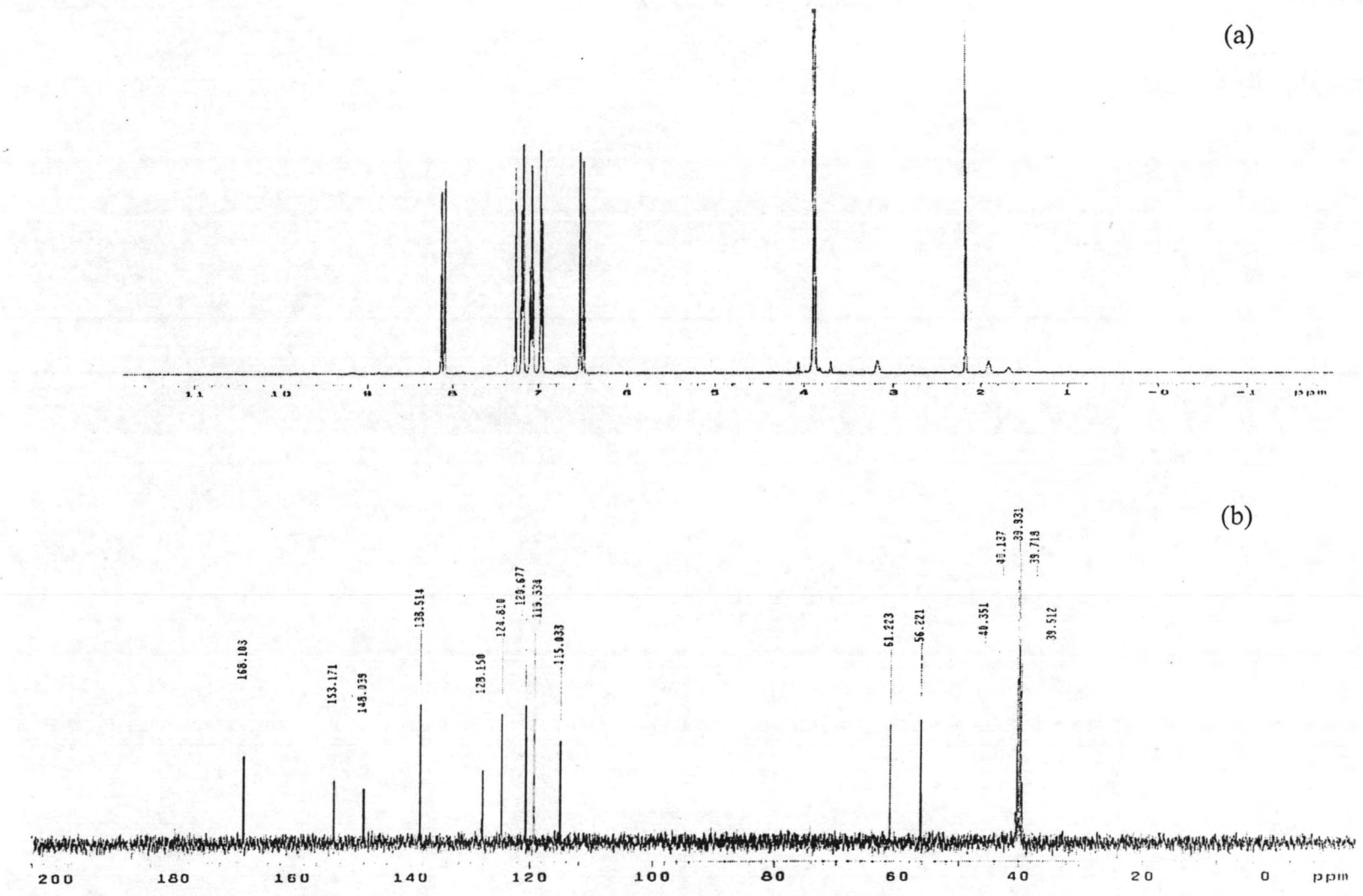

Figure A5 ^{1}H (a) and ^{13}C NMR spectrum (b) of 2,3-methoxycinnamic acid (**4A**) in DMSO-d_6.

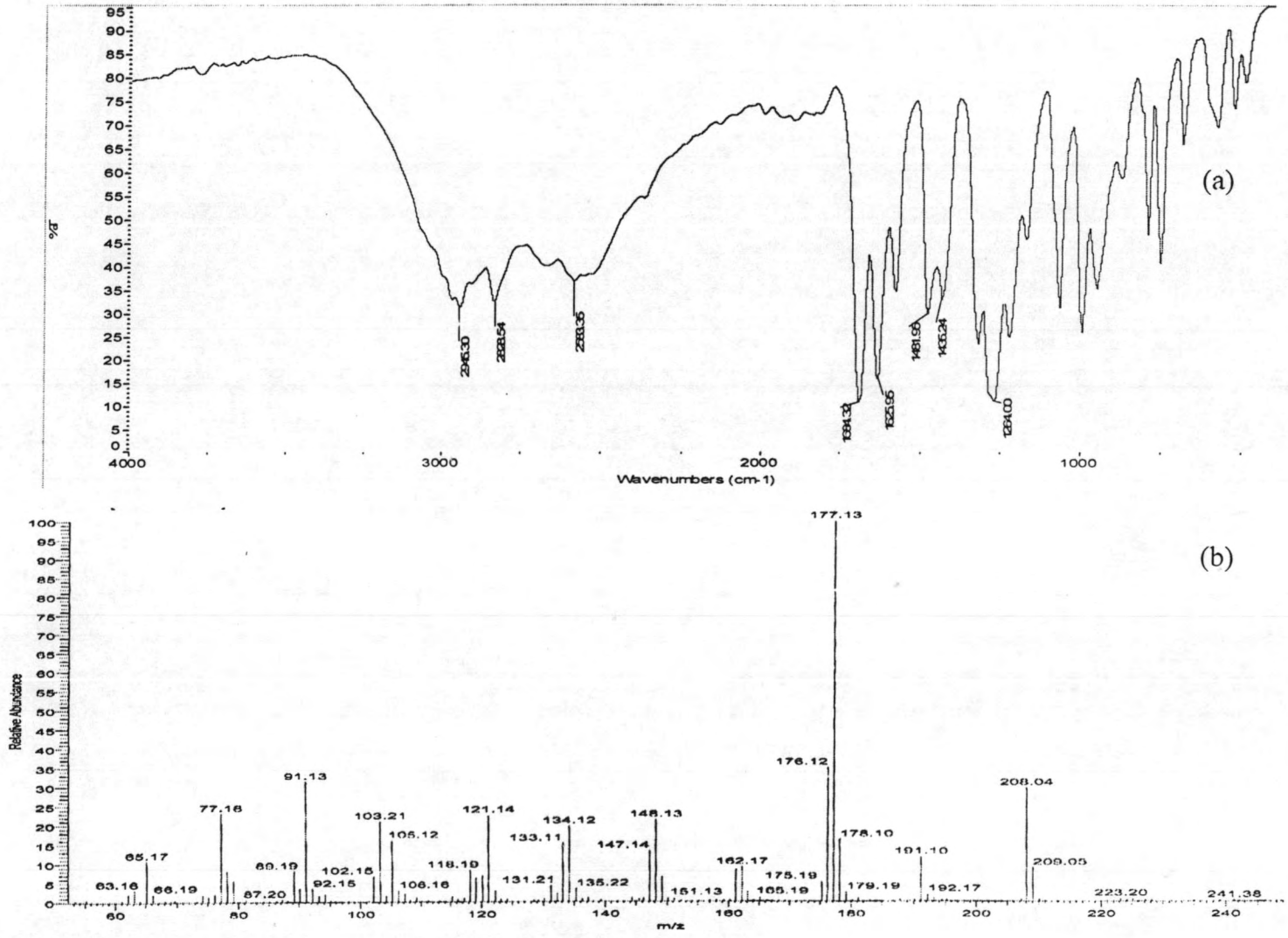

Figure A6 IR (a) and MS spectrum (b) of 2,3-methoxycinnamic acid (**4A**).

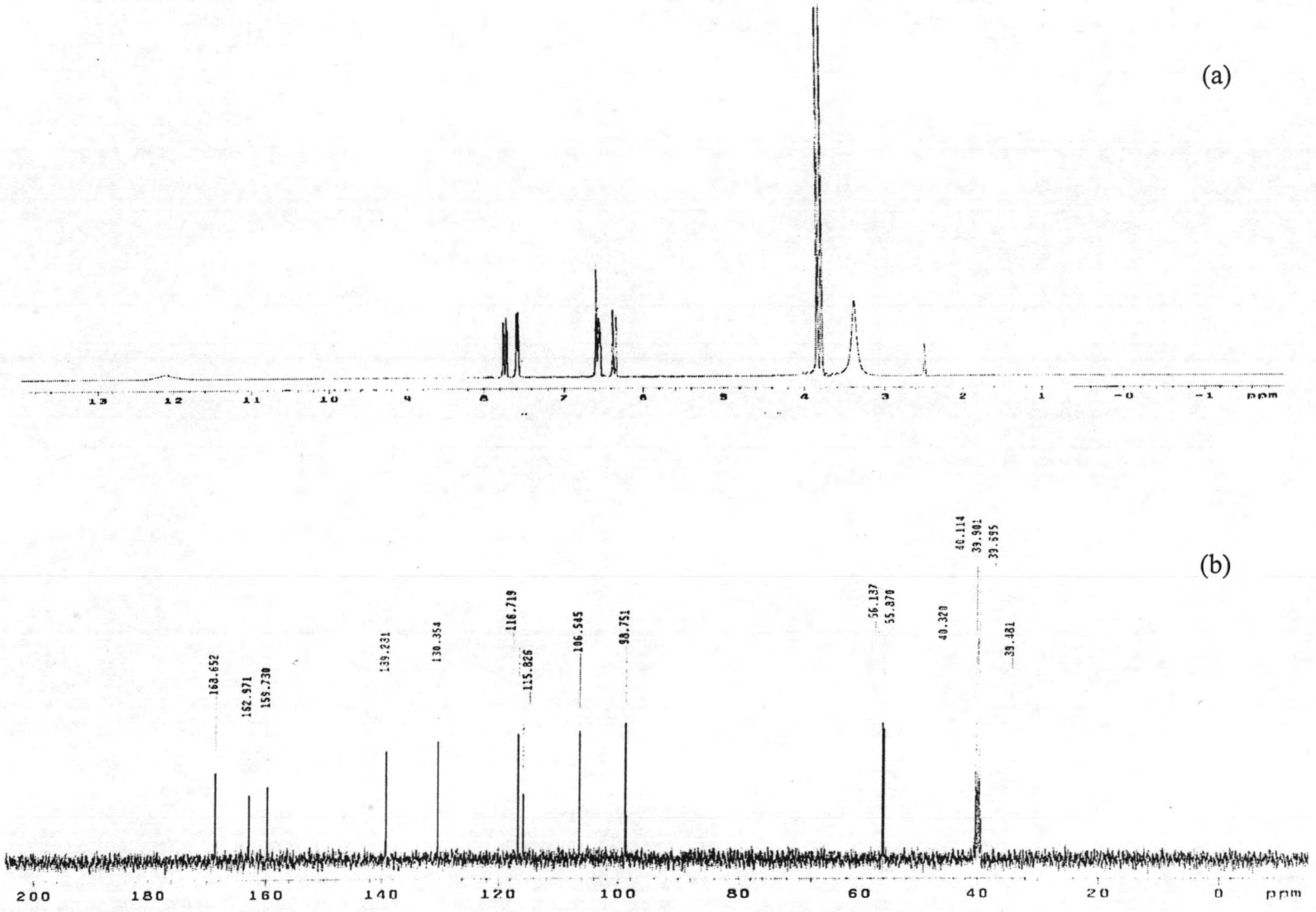

Figure A7 ^{1}H (a) and ^{13}C NMR spectrum (b) of 2,4-dimethoxycinnamic acid (**5A**) in DMSO-d_6.

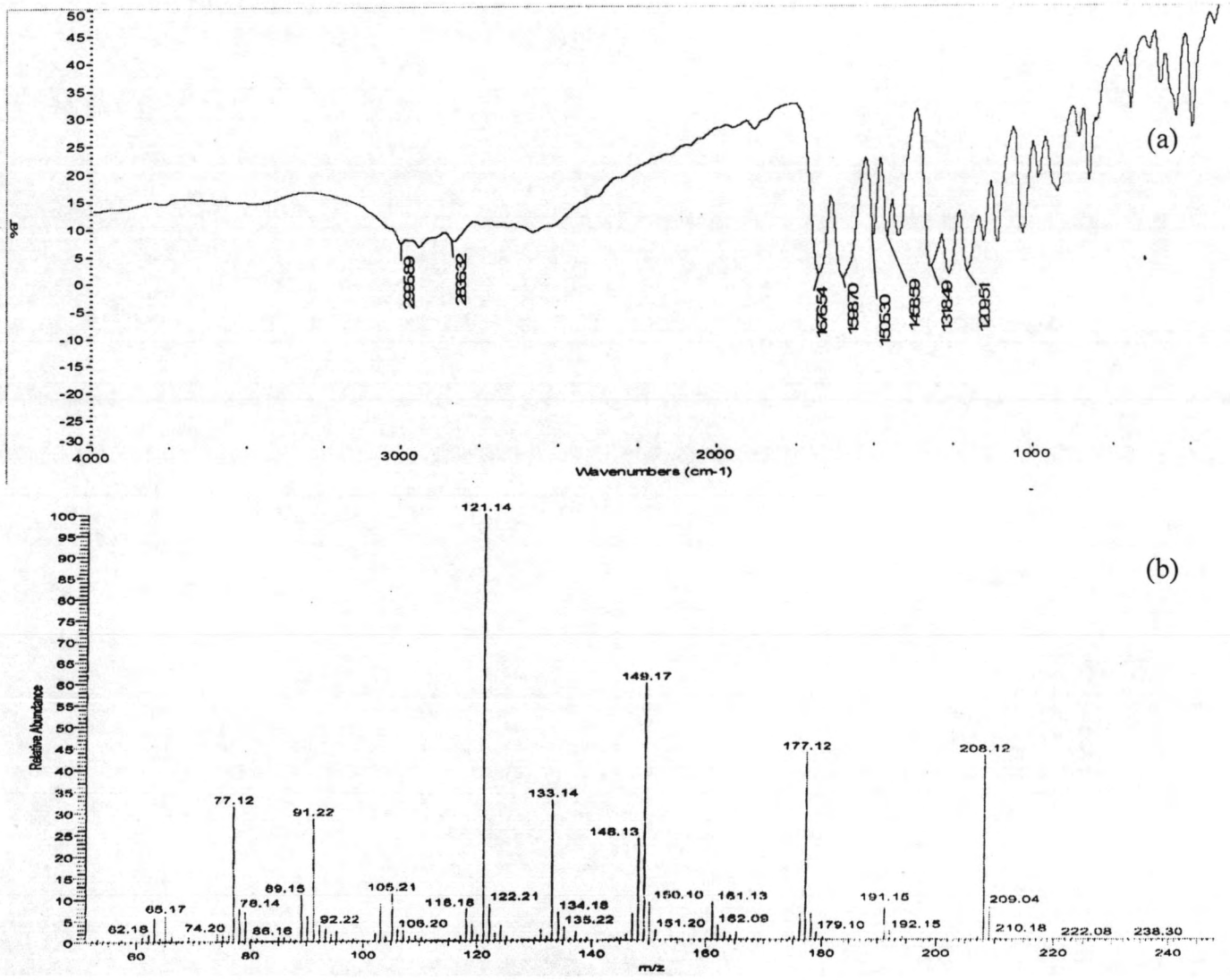

Figure A8 IR (a) and MS spectrum (b) of 2,4-methoxycinnamic acid **(5A)**.

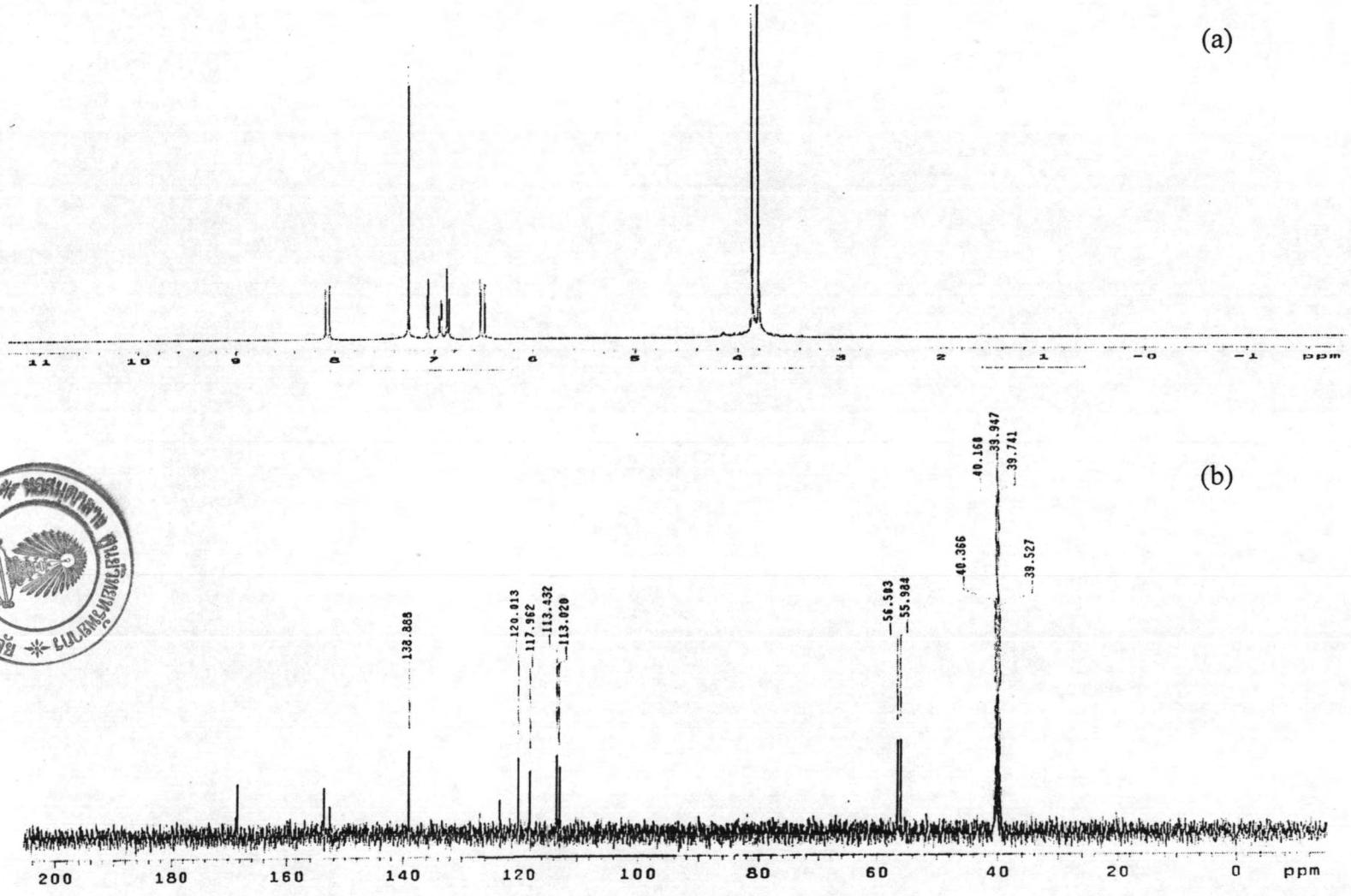

Figure A9 ^{1}H (a) and ^{13}C NMR spectrum (b) of 2,5-dimethoxycinnamic acid (**6A**) in $CDCl_3$ and DMSO-d_6, respectively.

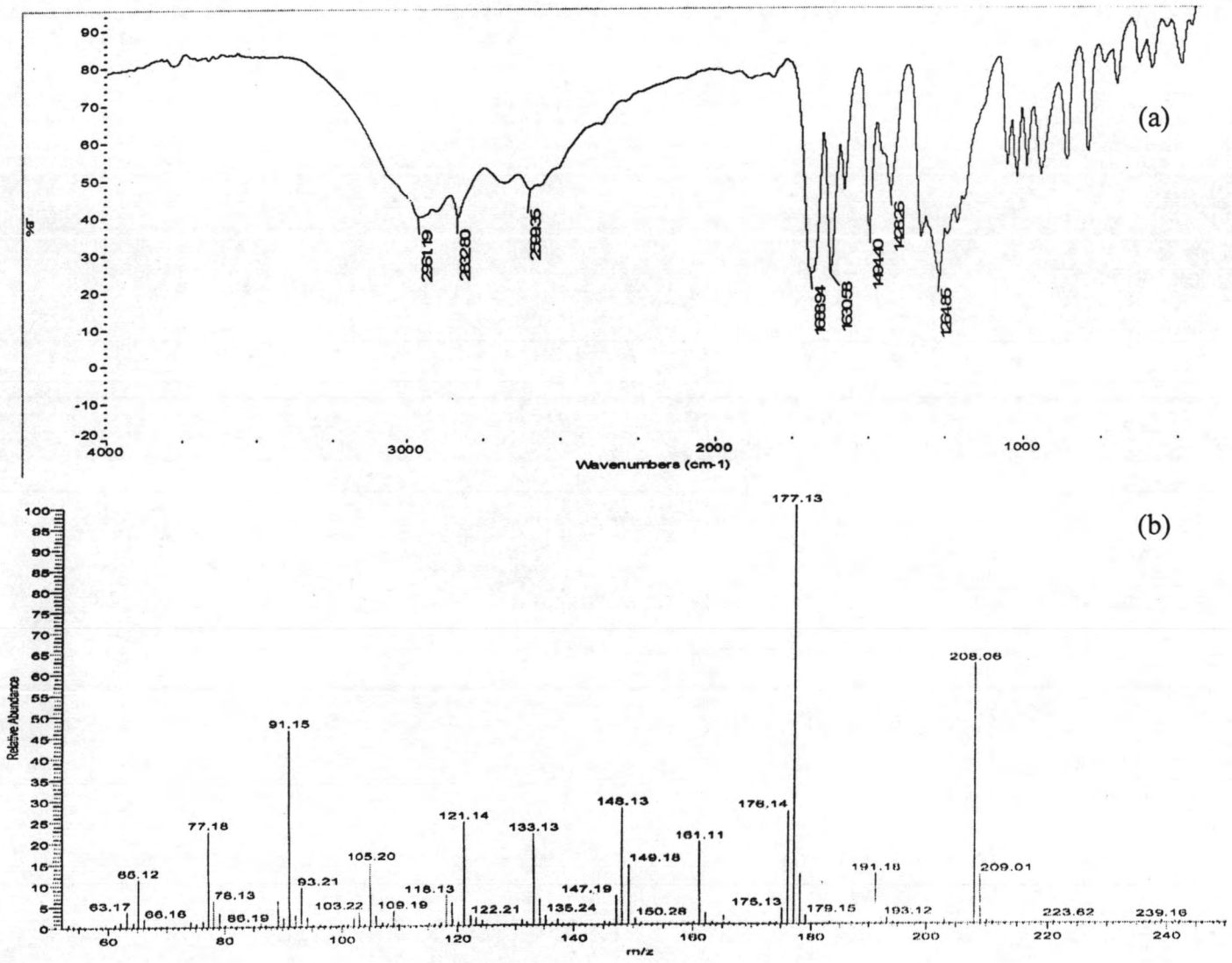

Figure A10 IR (a) and MS spectrum (b) of 2,5-methoxycinnamic acid **(5A)**.

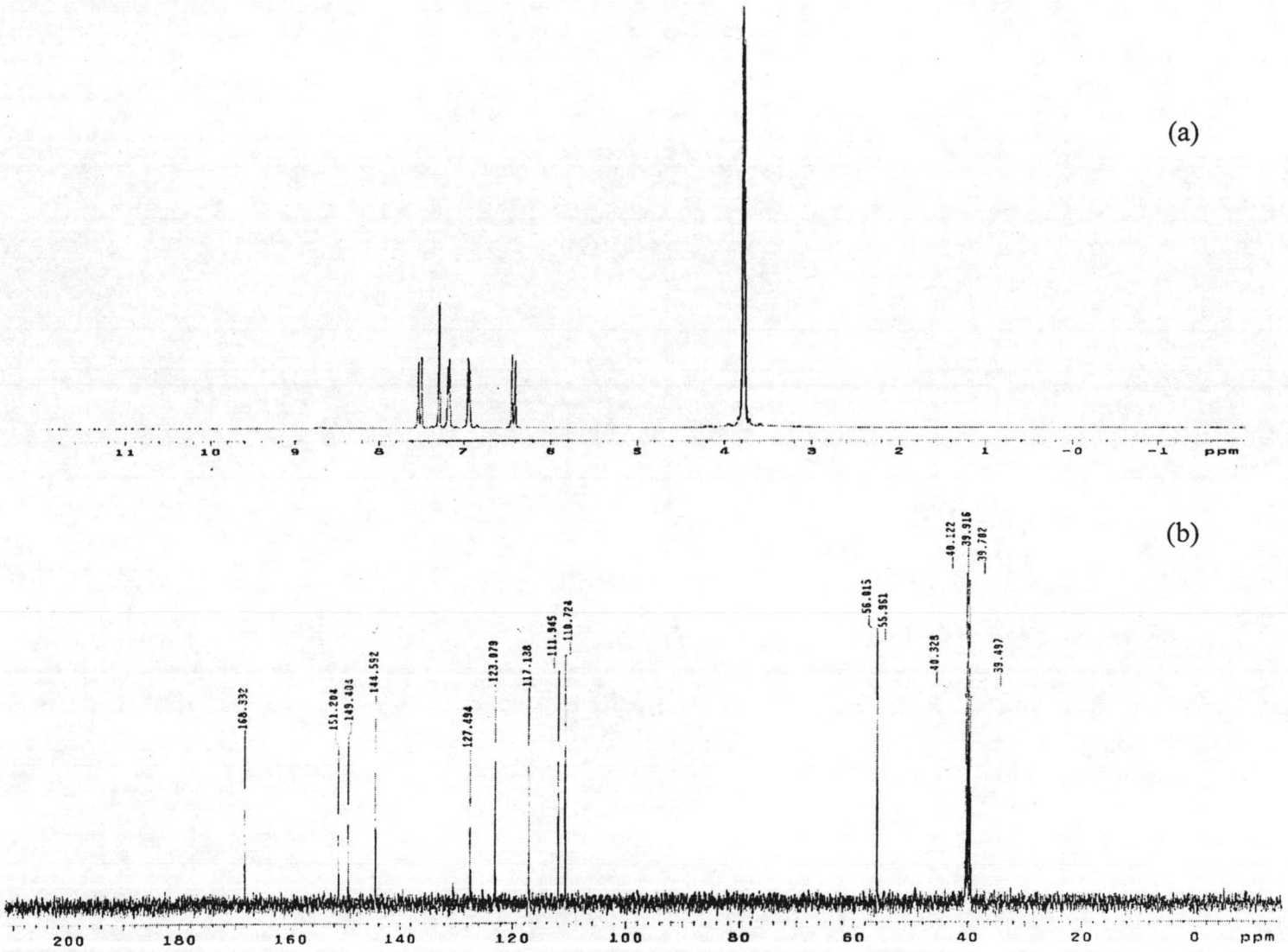

Figure A11 ^{1}H (a) and ^{13}C NMR spectrum (b) of 3,4-dimethoxycinnamic acid (**6A**) in DMSO-d_6.

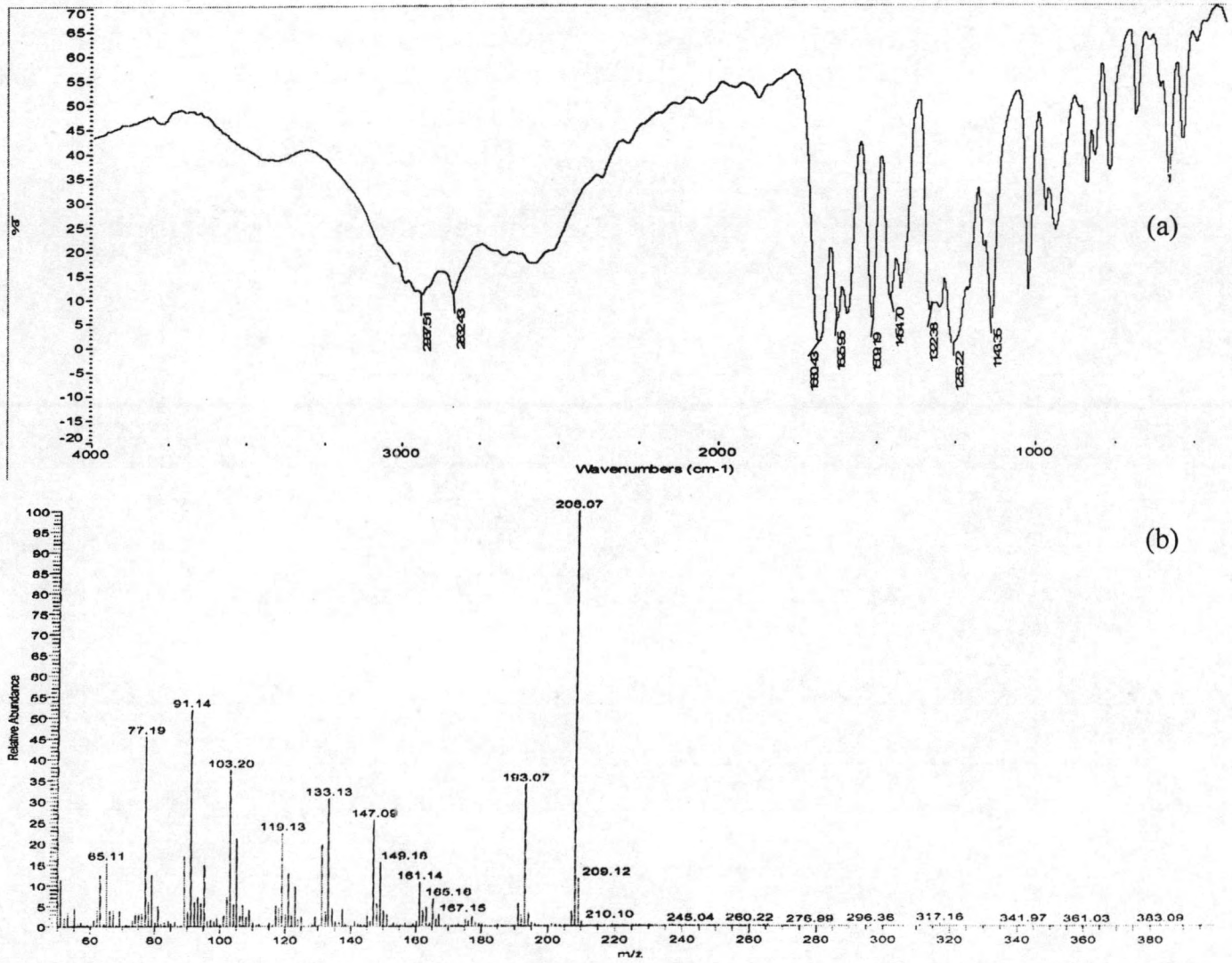

Figure A12 IR (a) and MS spectrum (b) of 3,4-methoxycinnamic acid (**6A**).

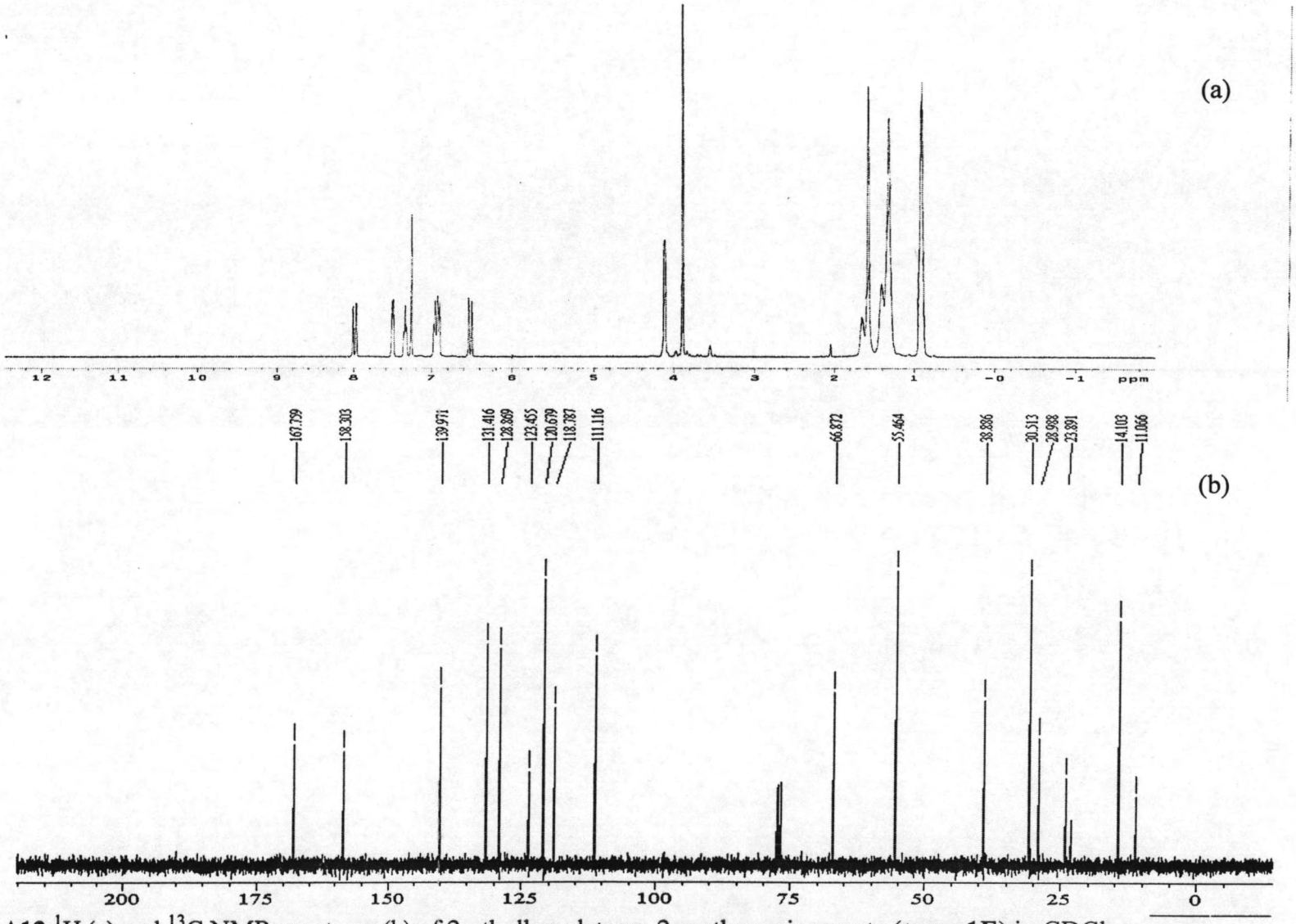

Figure A13 ^{1}H (a) and ^{13}C NMR spectrum (b) of 2-ethylhexyl-*trans*-2-methoxycinnamate (*trans*-**1E**) in $CDCl_3$.

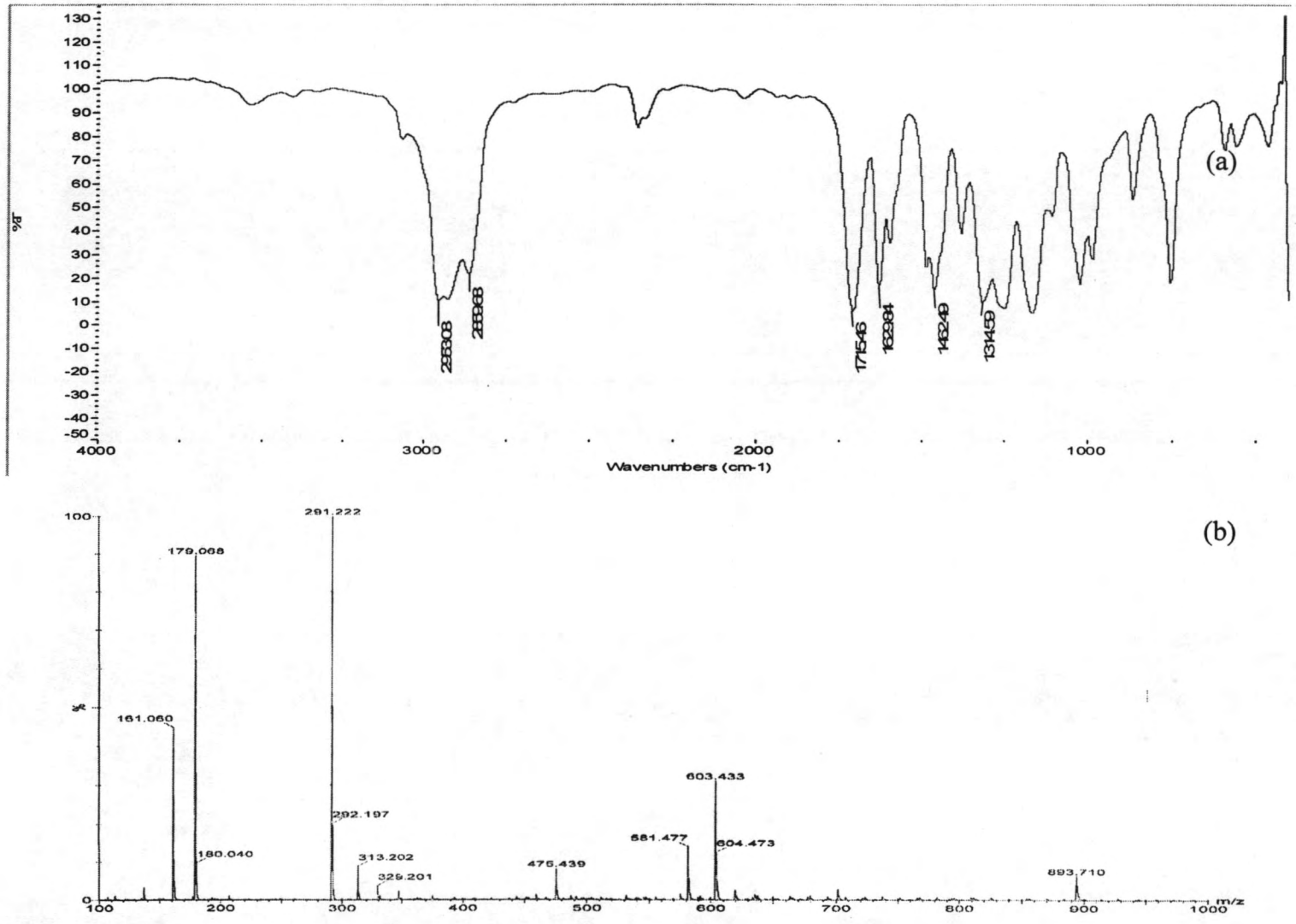

Figure A14 IR (a) and MS spectrum (b) of 2-ethylhexyl-*trans*-2-methoxycinnamate (*trans*-**1E**).

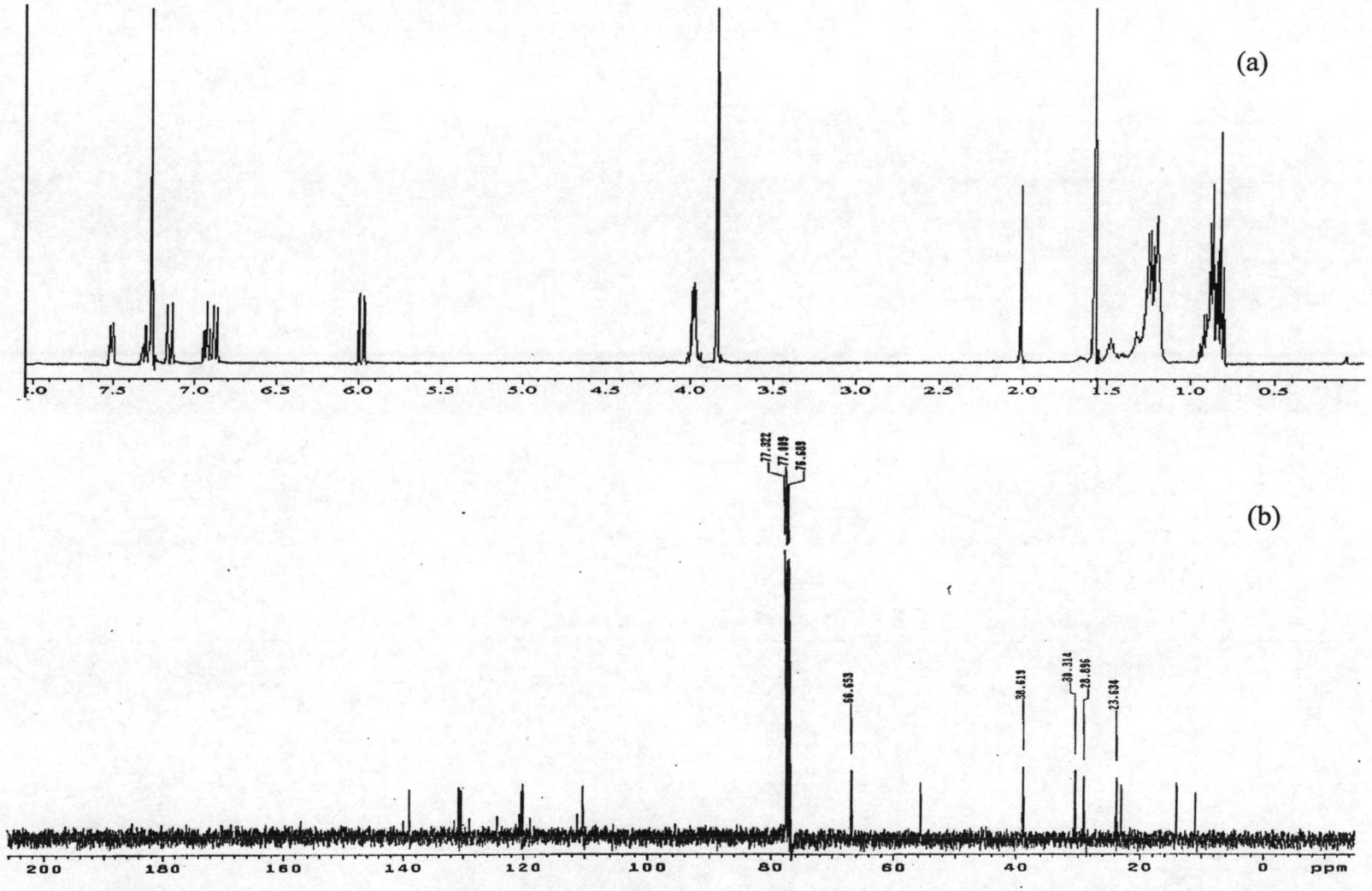

Figure A15 ^{1}H (a) and ^{13}C NMR spectrum (b) of 2-ethylhexyl-*cis*-2-methoxycinnamate (*cis*-**1E**).in $CDCl_3$.

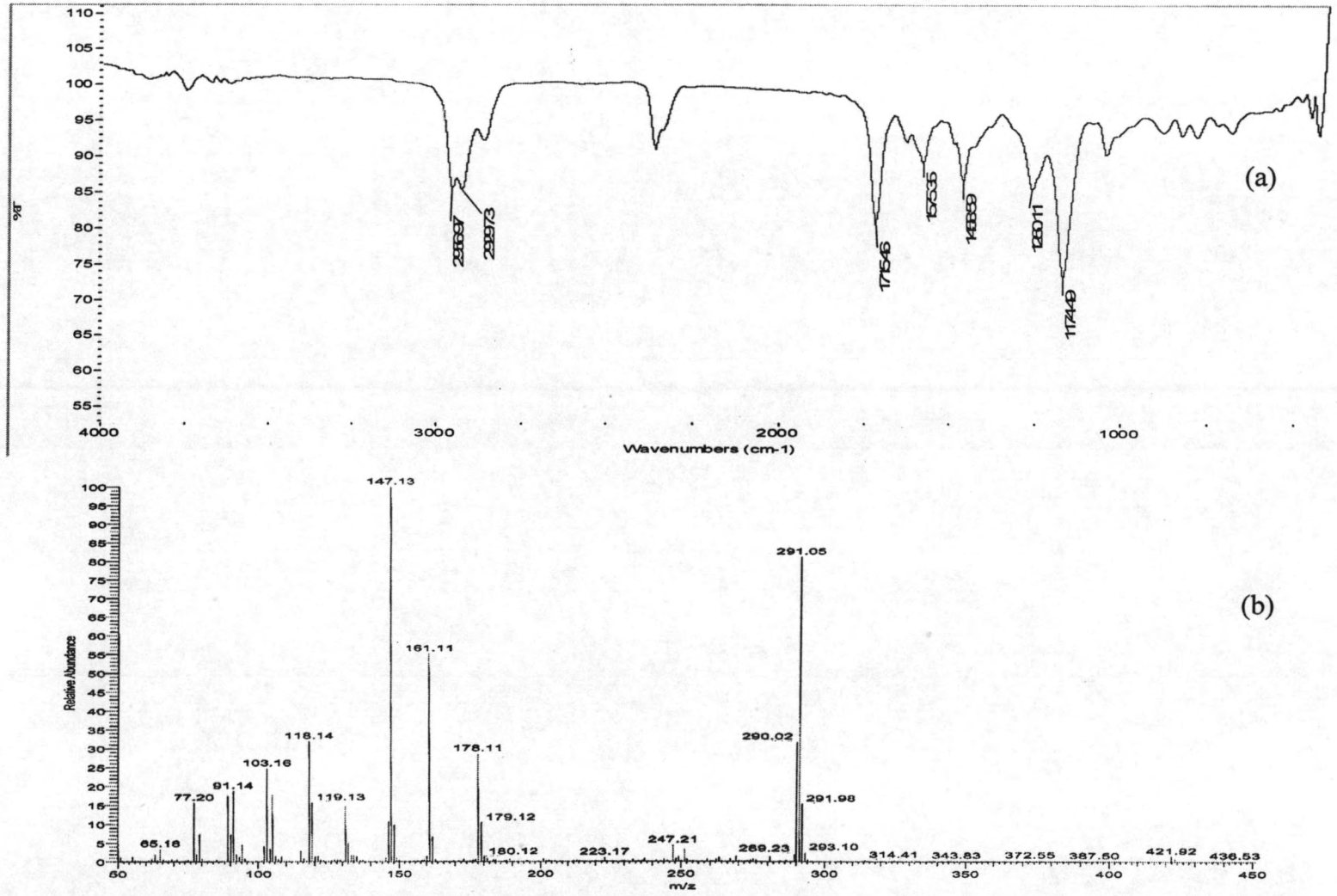

Figure A16 IR (a) and MS spectrum (b) of 2-ethylhexyl-*cis*-2-methoxycinnamate (*cis*-**1E**).

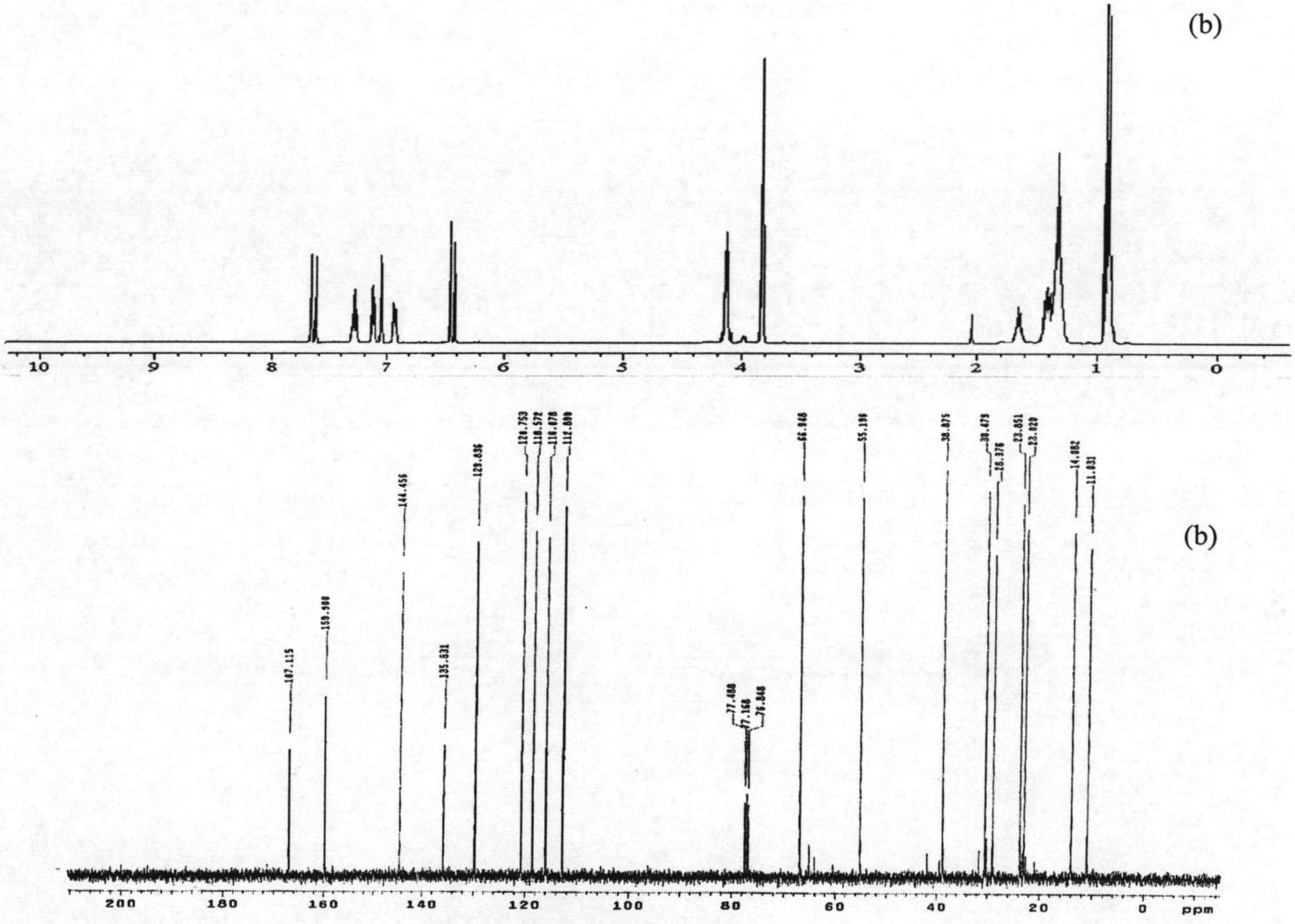

Figure A17 ^{1}H (a) and ^{13}C NMR spectrum (b) of 2-ethylhexyl-*trans*-3-methoxycinnamate (*trans*-**2E**) in $CDCl_3$.

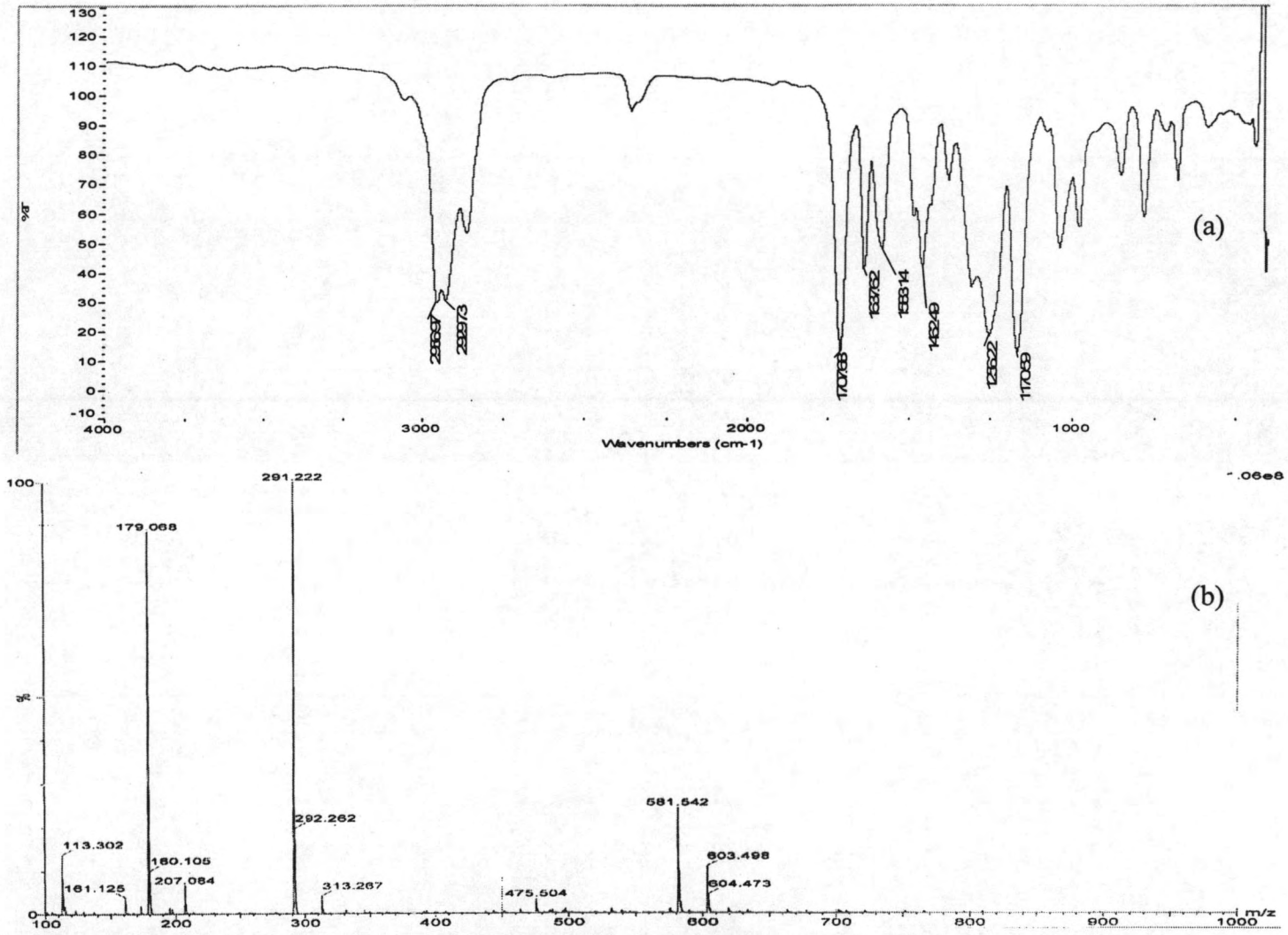

Figure A18 IR (a) and MS spectrum (b) of 2-ethylhexyl-*trans*-3-methoxycinnamate (*trans*-**2E**).

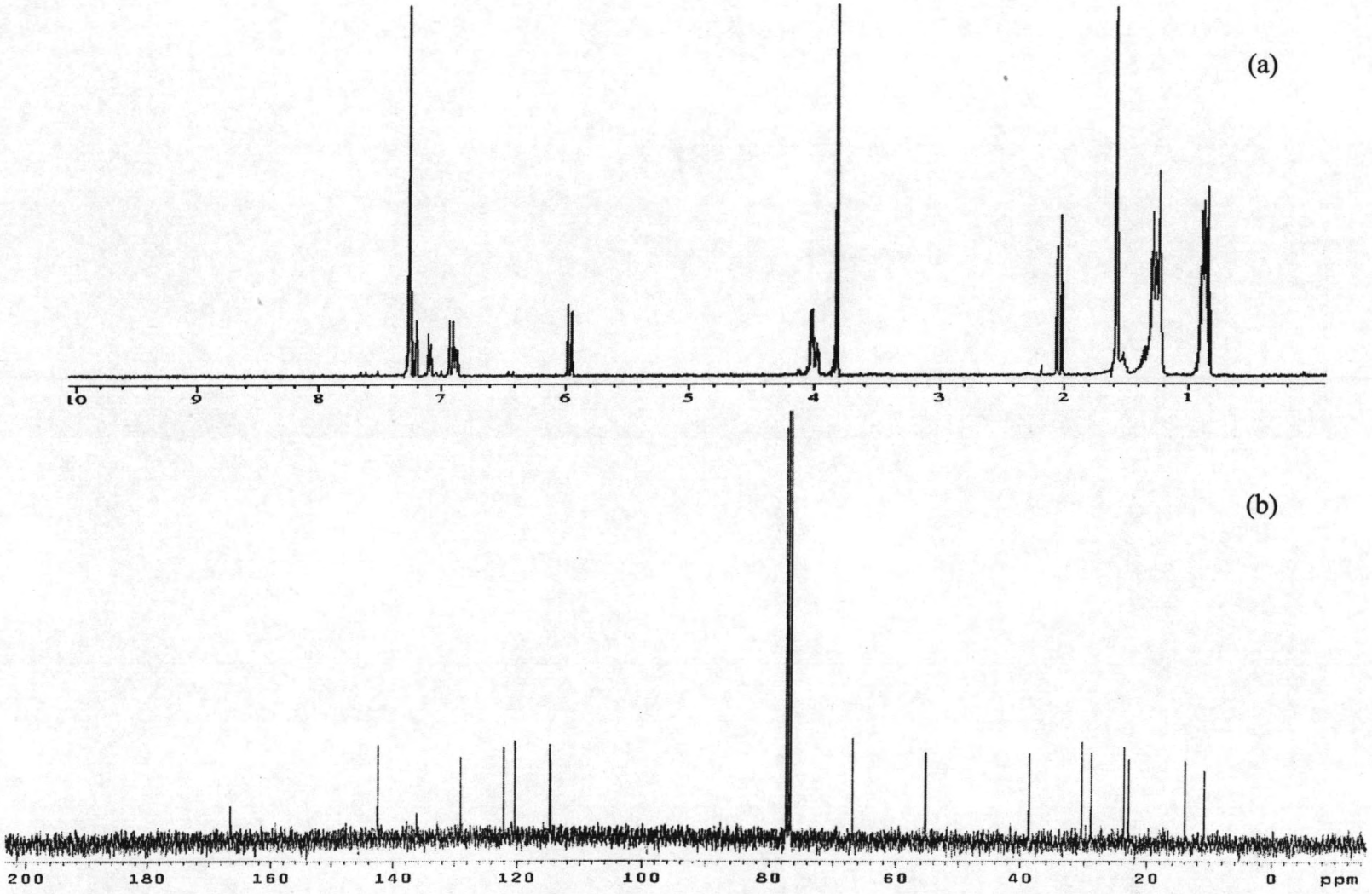

Figure A19 ^{1}H (a) and ^{13}C NMR spectrum (b) of 2-ethylhexyl-*cis*-3-methoxycinnamate (*cis*-**2E**) in $CDCl_3$.

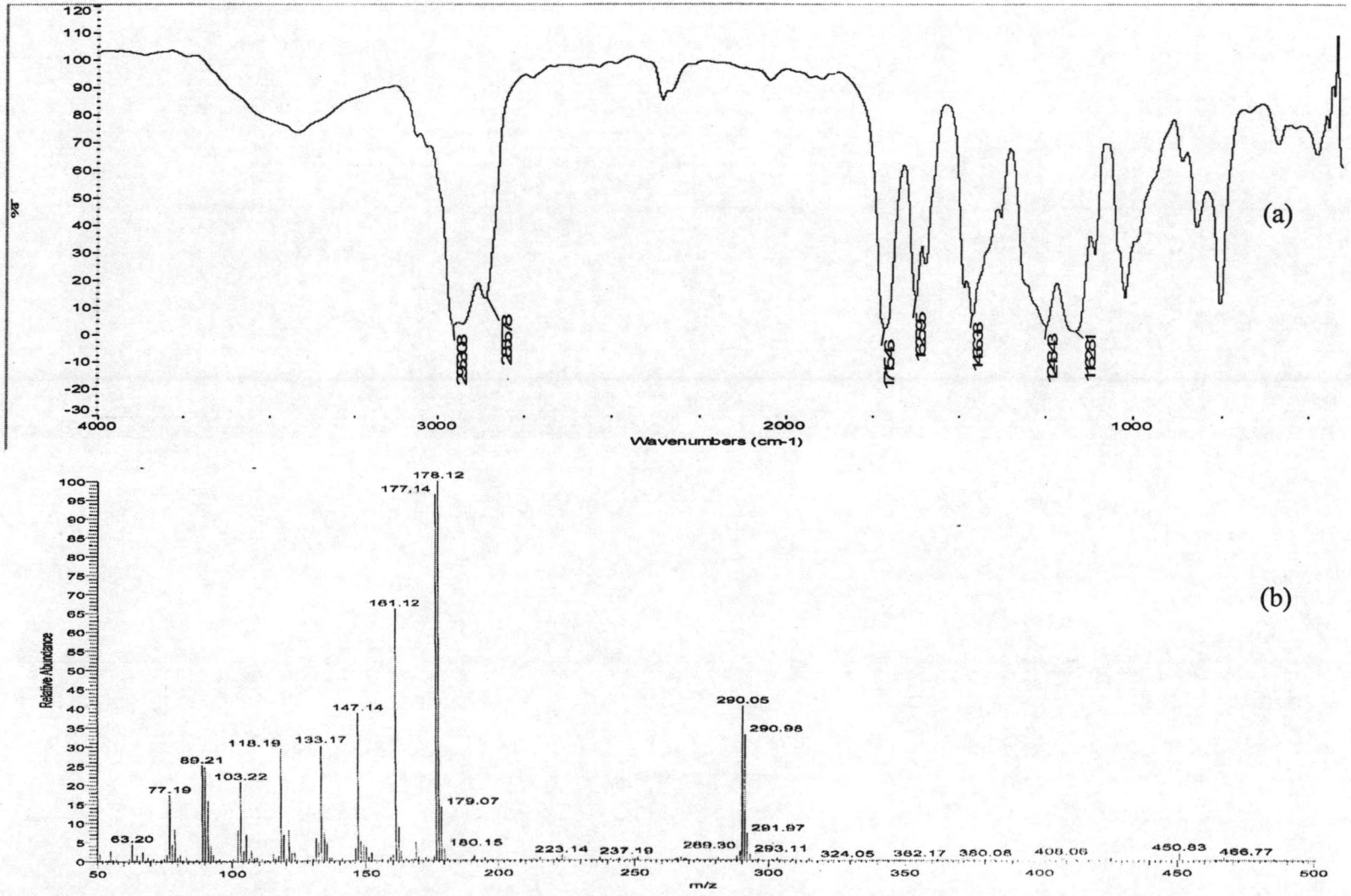

Figure A20 IR (a) and MS spectrum (b) of 2-ethylhexyl-*cis*-3-methoxycinnamate (*cis*-**2E**).

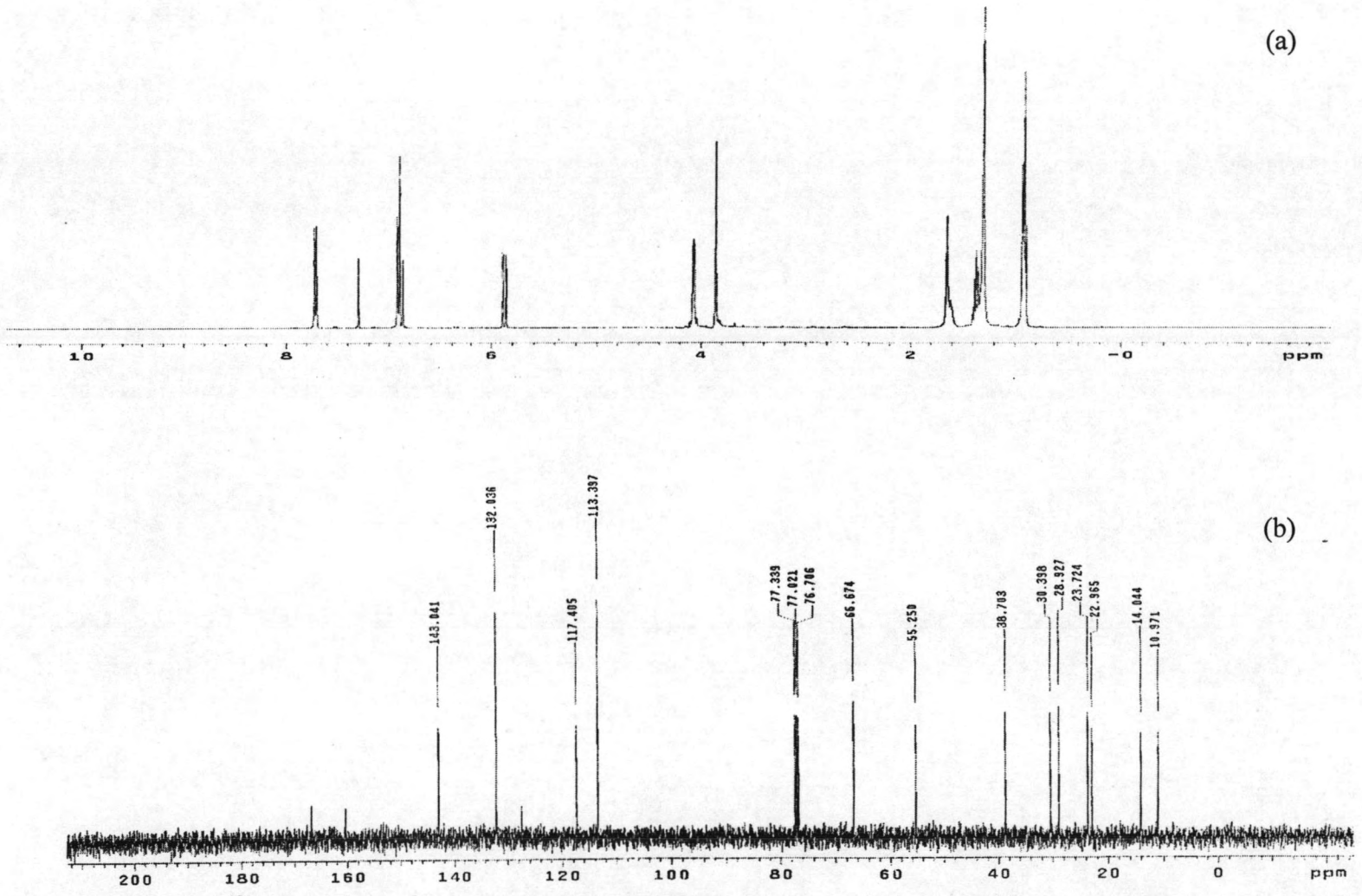

Figure A21 ^{1}H (a) and ^{13}C-NMR spectrum (b) spectrum of 2-ethylhexyl-*cis*-4-methoxycinnamate (*cis*-**3E**).

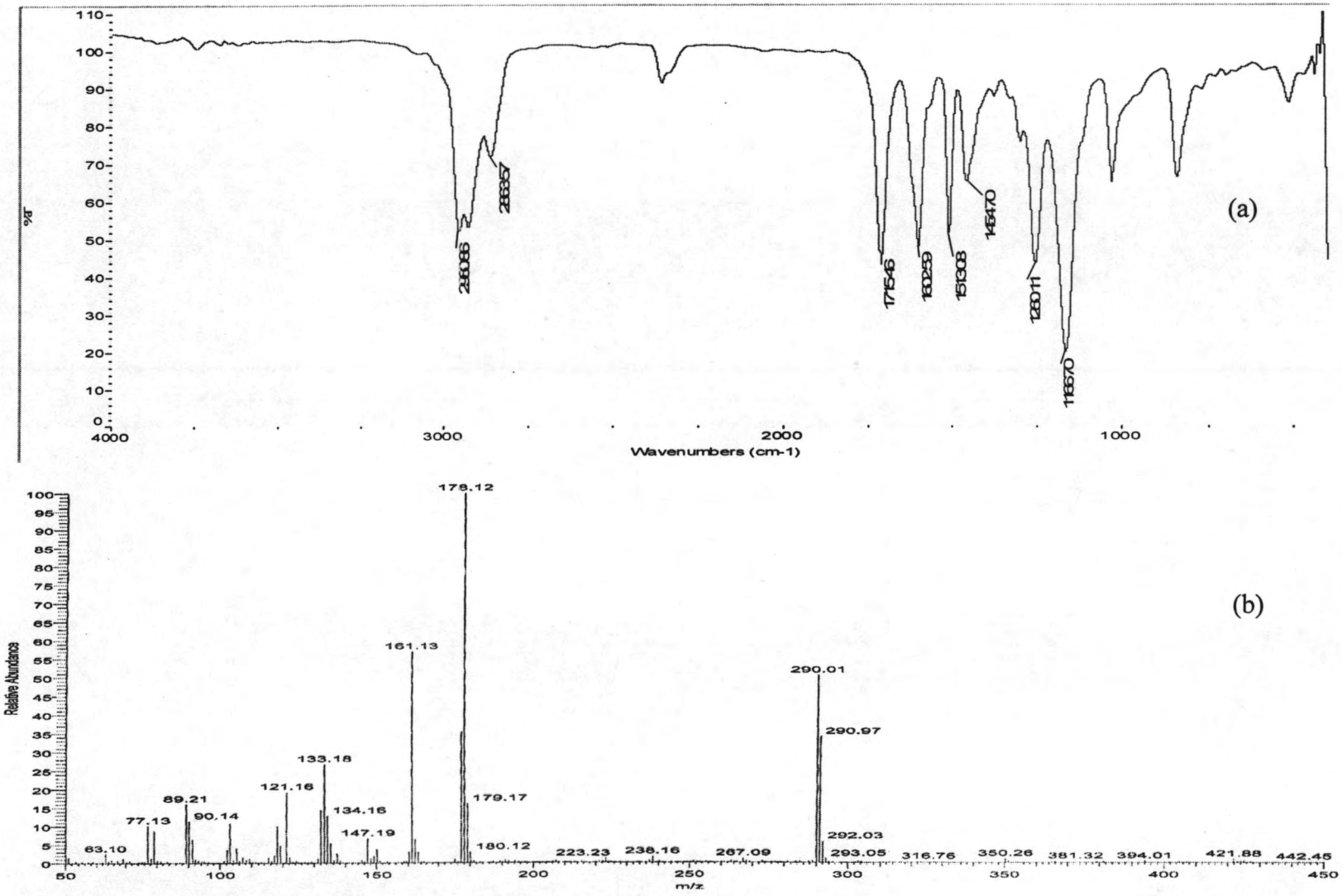

Figure A22 IR (a) and MS spectrum (b) of 2-ethylhexyl-*cis*-4-methoxycinnamate (*cis*-**3E**).

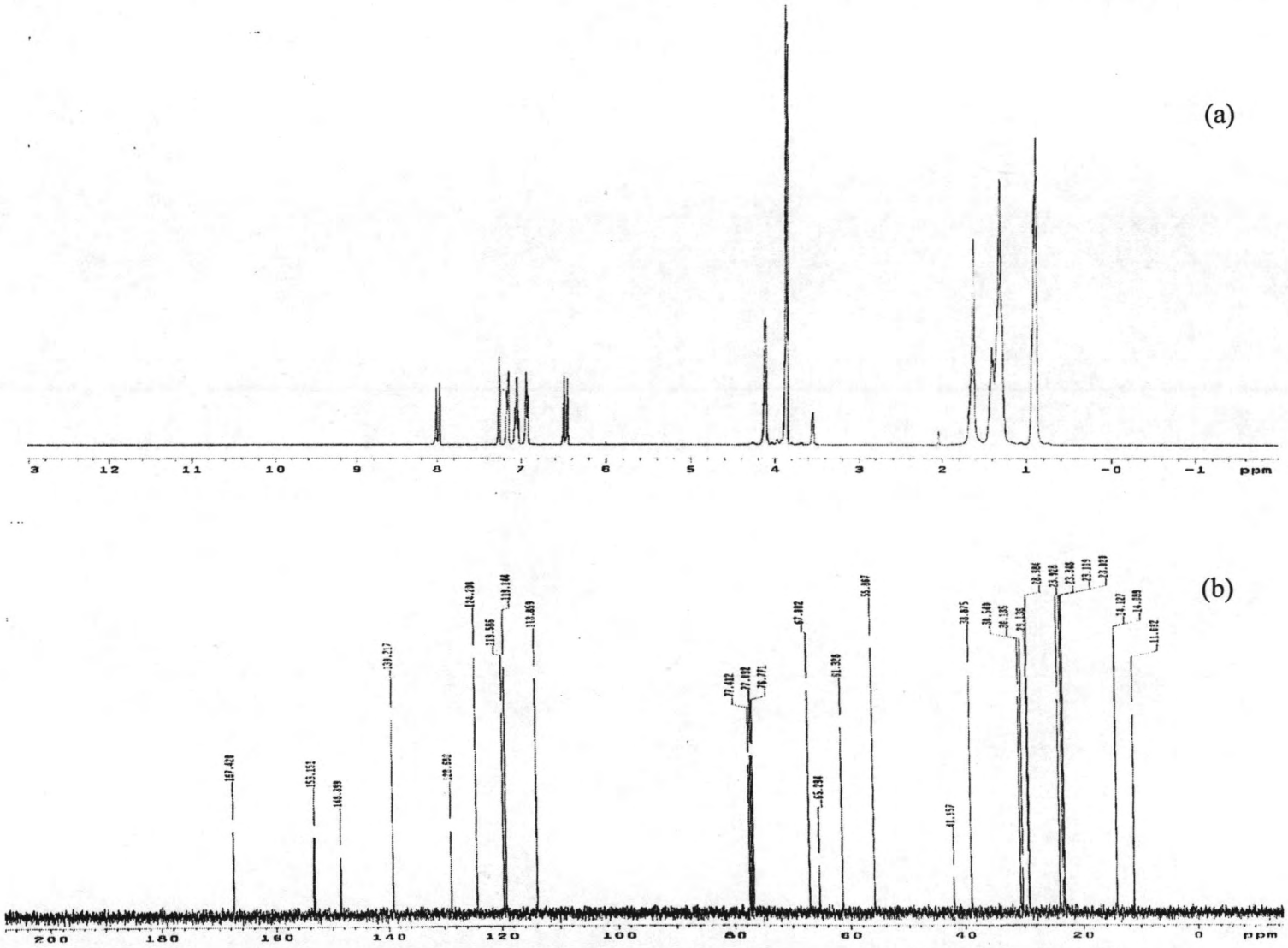

Figure A23 ^{1}H (a) and ^{13}C NMR spectrum (b) of 2-ethylhexyl-*trans*-2,3-trimethoxycinnamate (*trans*-**4E**)in $CDCl_3$.

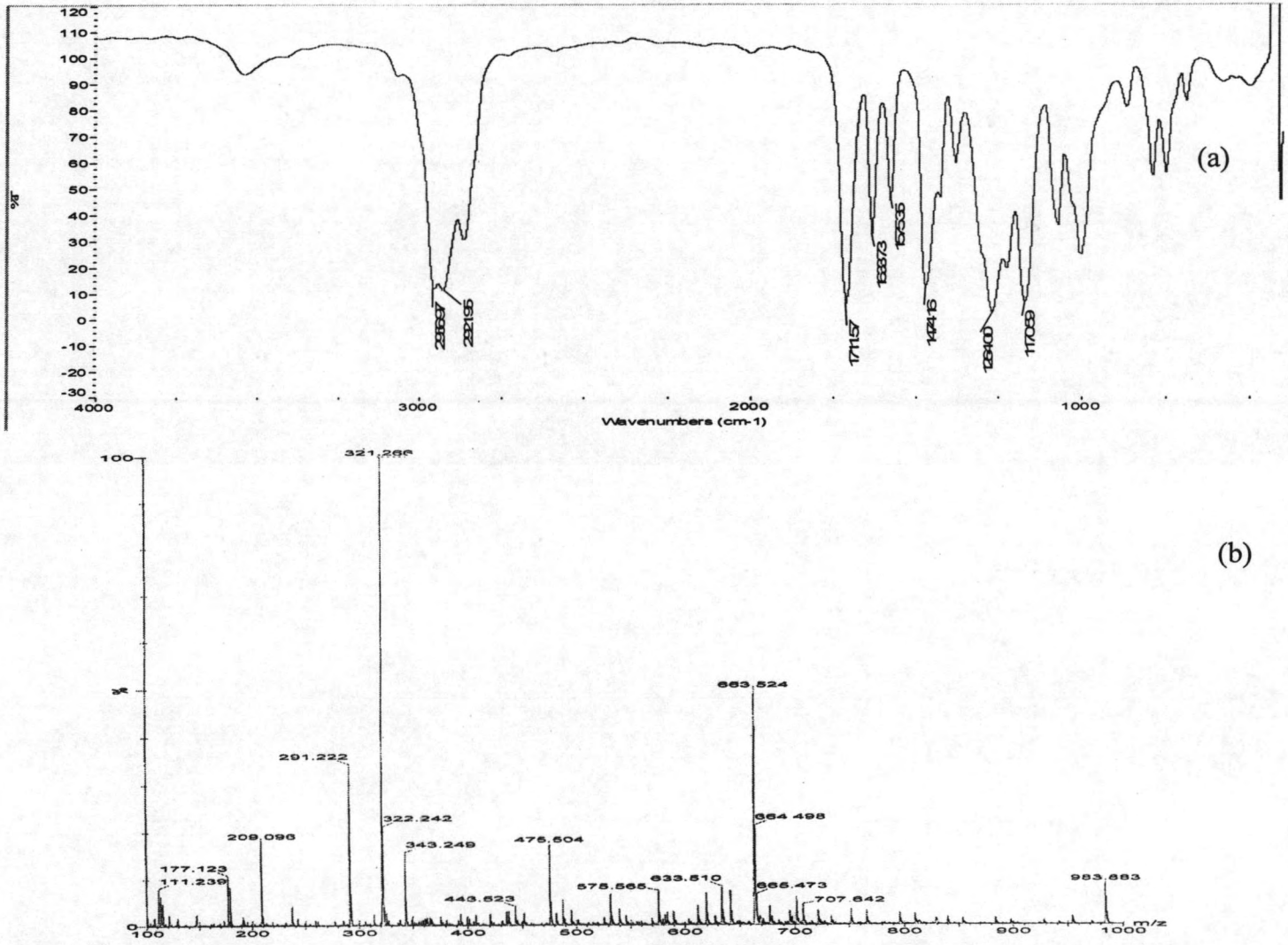

Figure A24 IR (a) and MS spectrum (b) of 2-ethylhexyl-*trans*-2,3-methoxycinnamate (*trans*-**4E**).

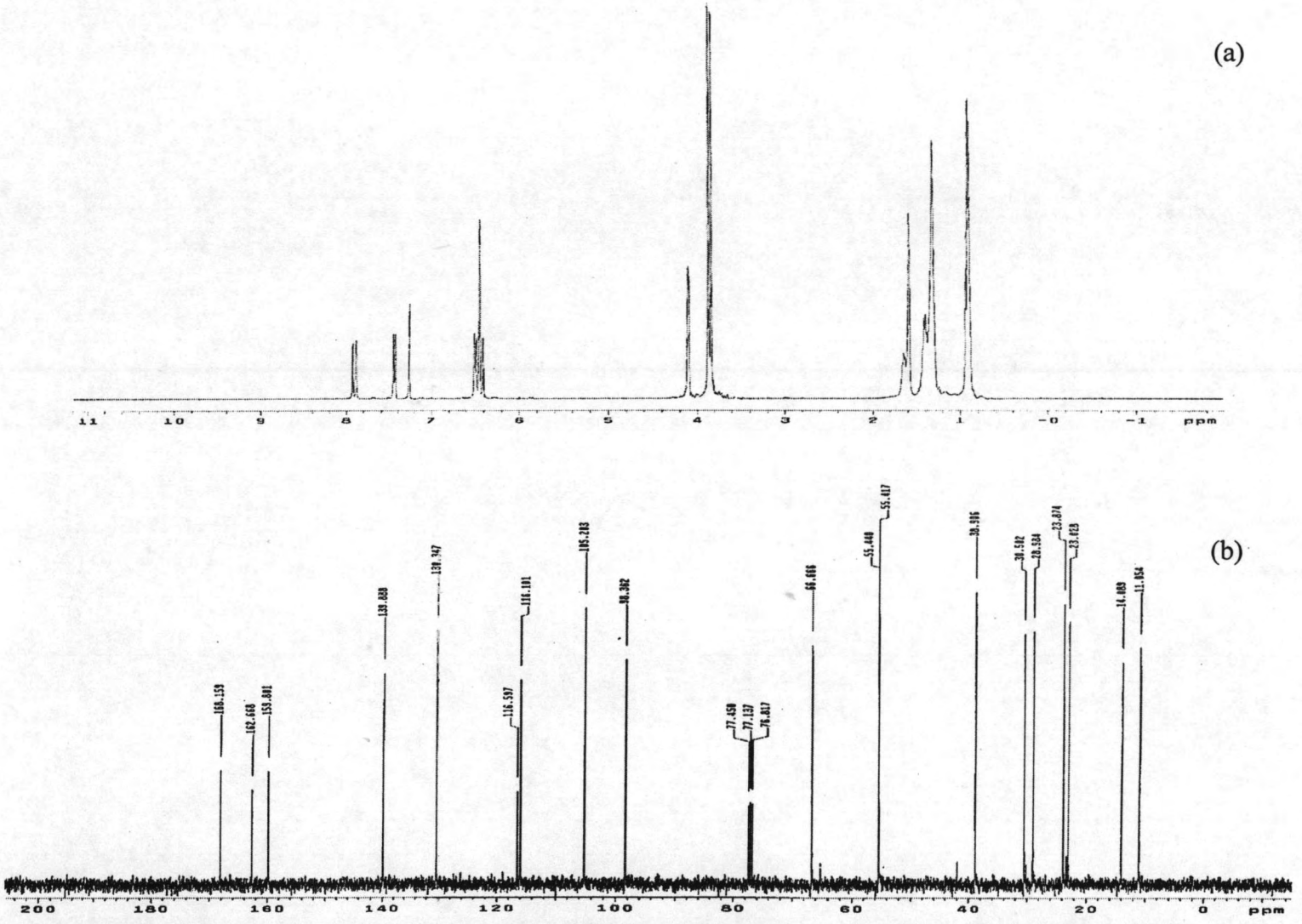

Figure A25 ^{1}H (a) and ^{13}C NMR spectrum (b) of 2-ethylhexyl-*trans*-2,4-dimethoxycinnamate (*trans*-**5E**) in $CDCl_3$

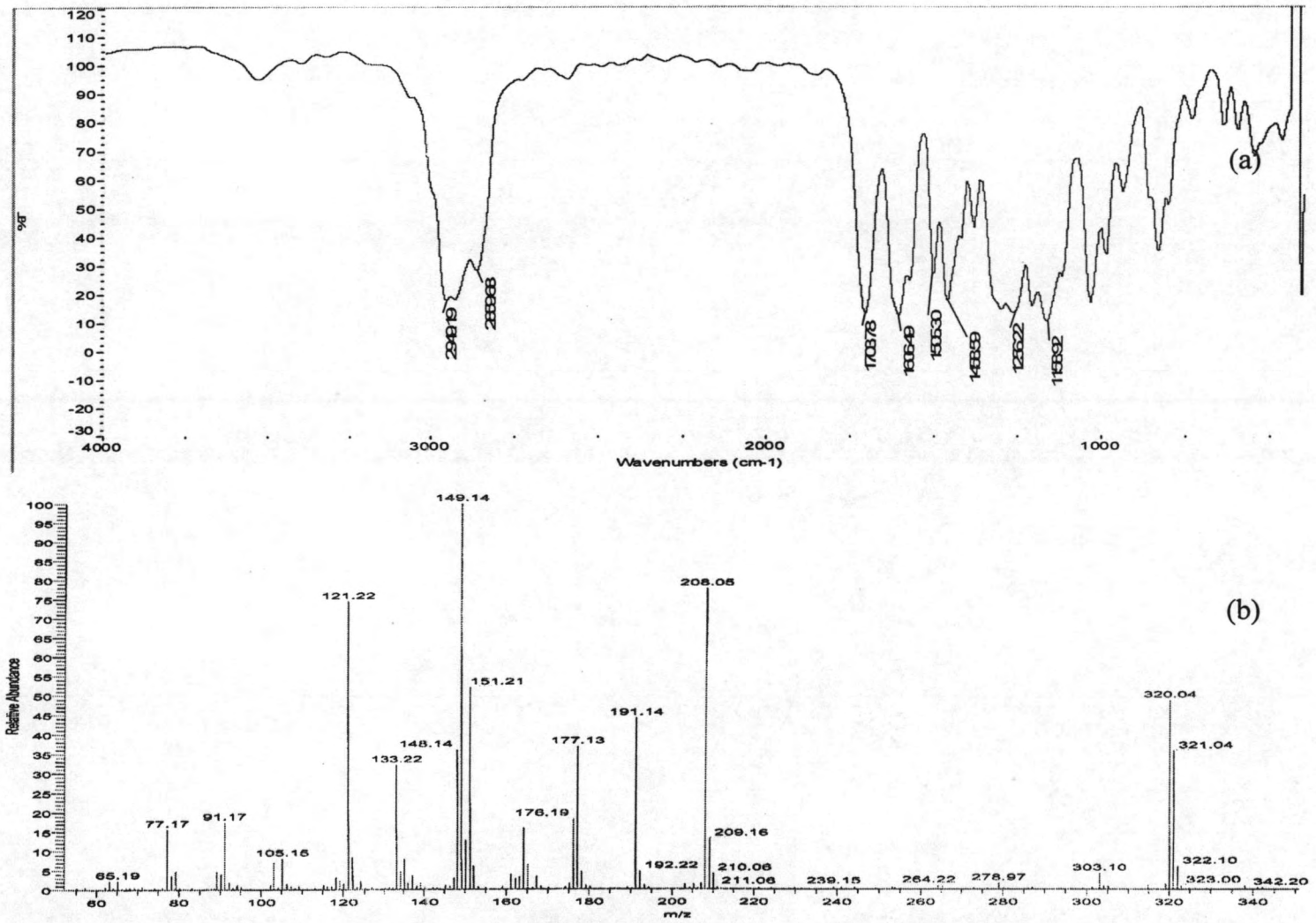

Figure A26 IR (a) and MS spectrum (b) of 2-ethylhexyl-*trans*-2,4-methoxycinnamate (*trans*-**5E**).

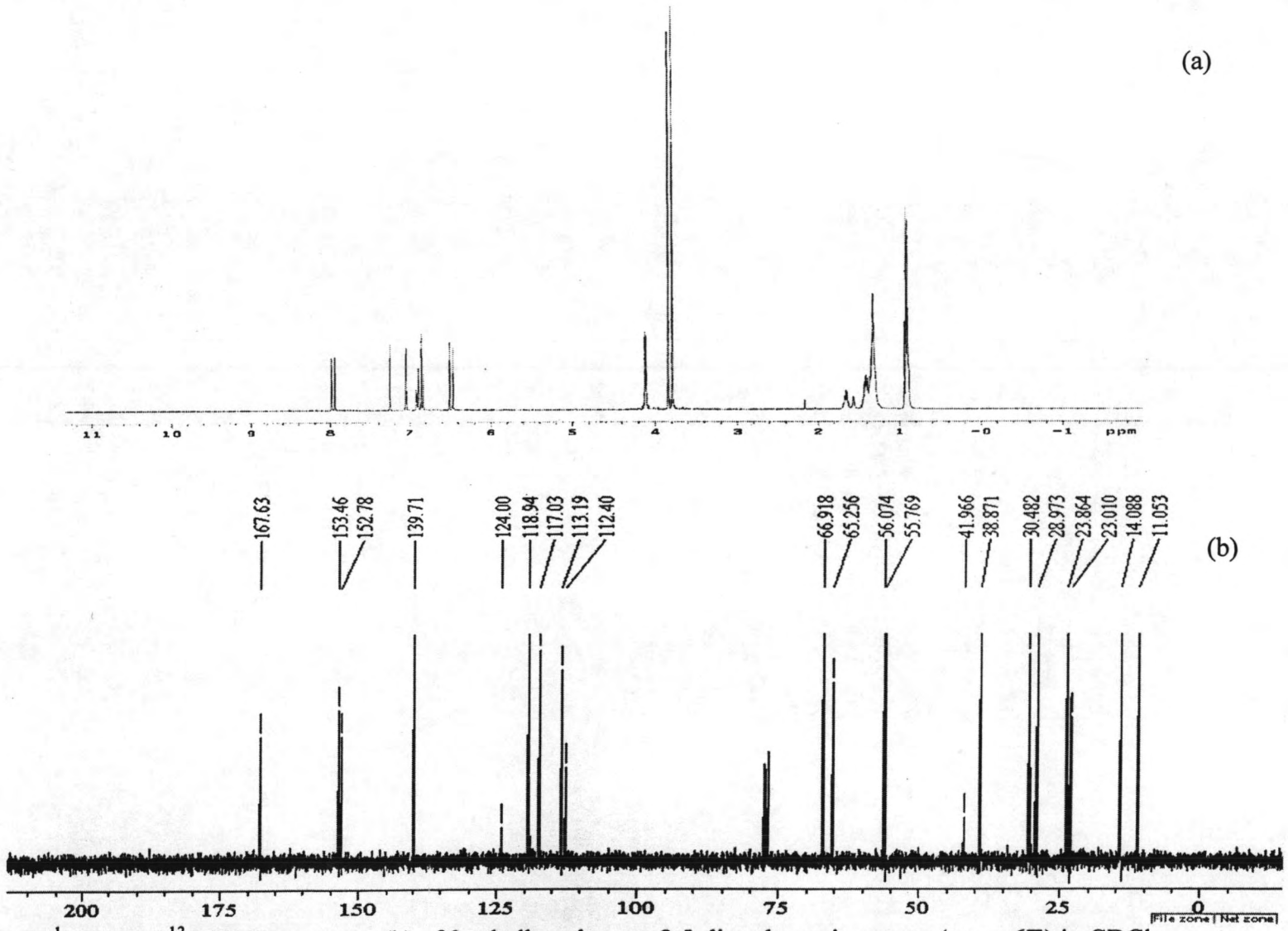

Figure A27 ^{1}H (a) and ^{13}C NMR spectrum (b) of 2-ethylhexyl-*trans*-2,5-dimethoxycinnamate (*trans*-**6E**) in $CDCl_3$.

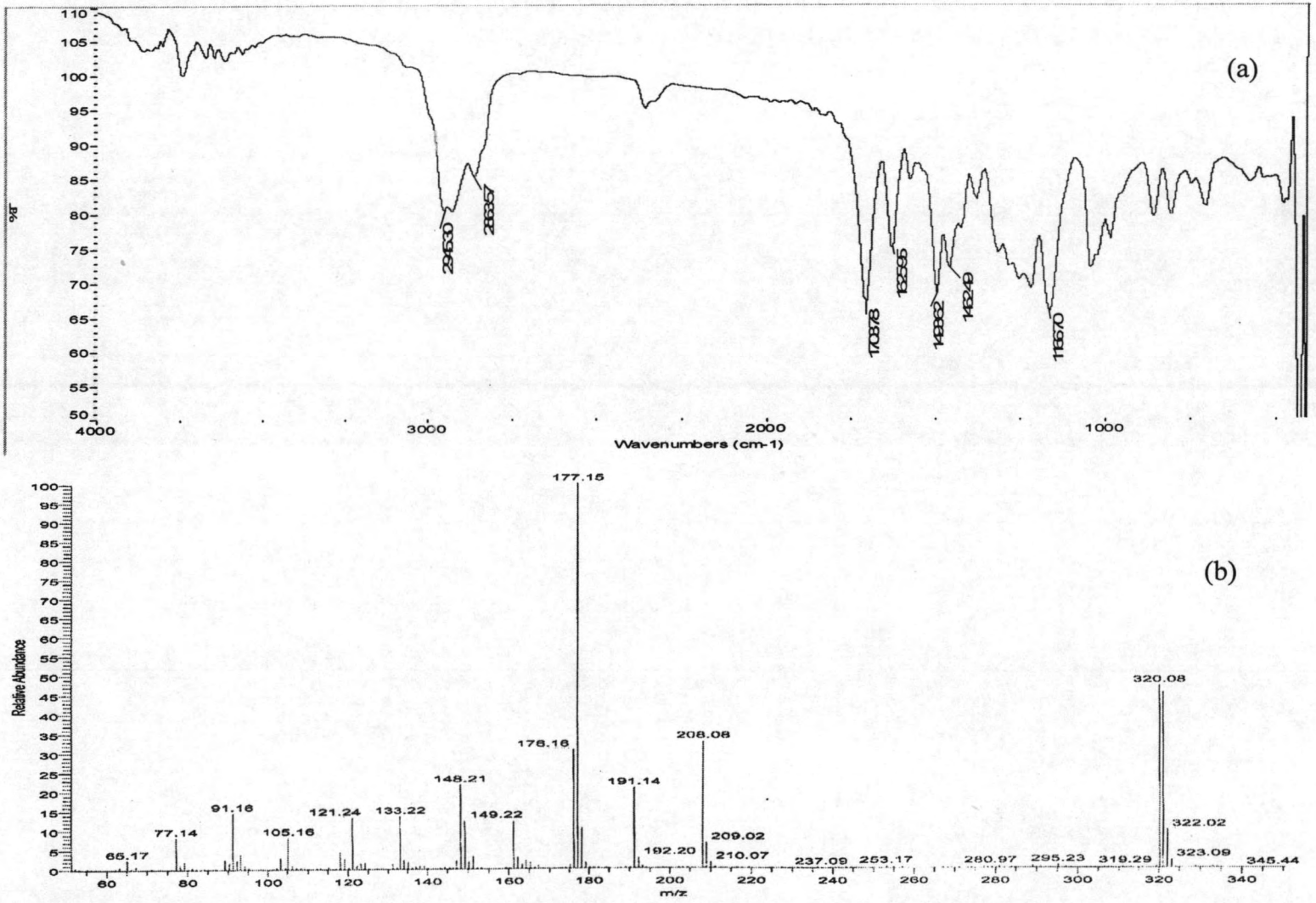

Figure A28 IR (a) and MS spectrum (b) of 2-ethylhexyl-*trans*-2,5-methoxycinnamate (*trans*-**6E**).

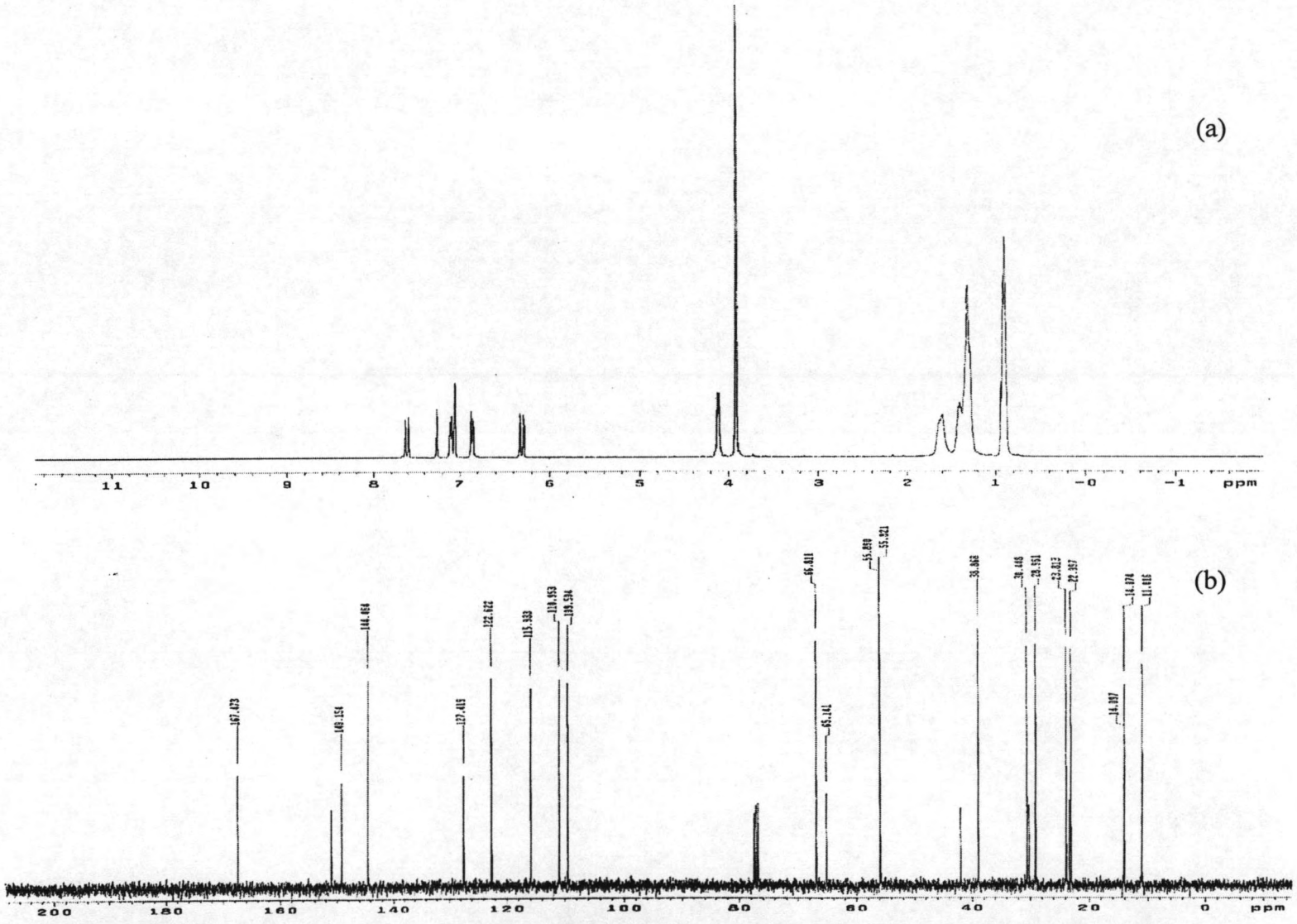

Figure A29 ^{1}H (a) and ^{13}C NMR spectrum (b) of 2-ethylhexyl-*trans*-3,4-dimethoxycinnamate (*trans*-**7E**) in $CDCl_3$.

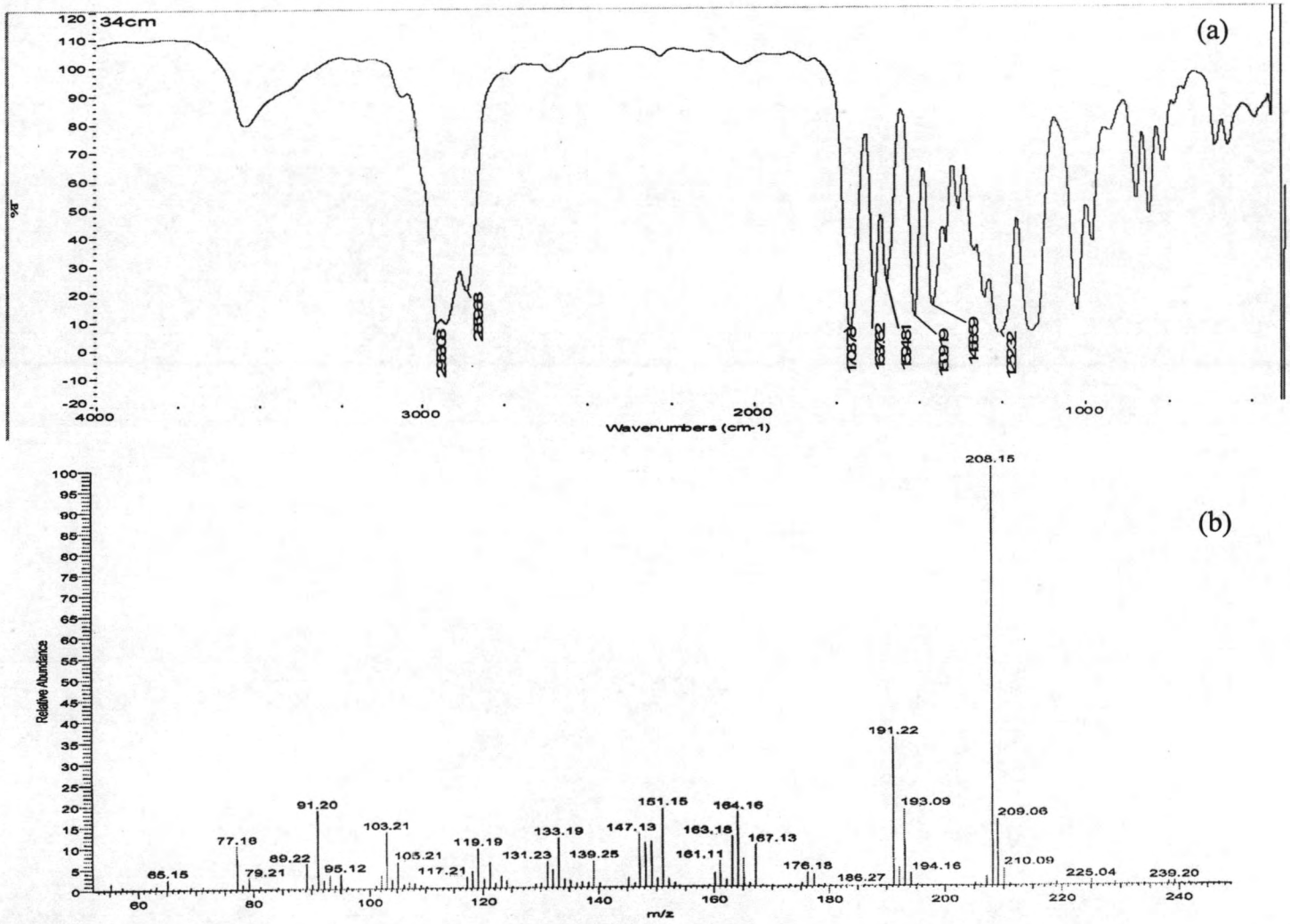

Figure A30 IR (a) and MS spectrum (b) of 2-ethylhexyl-*trans*-3,4-dimethoxycinnamate (*trans*-**7E**).

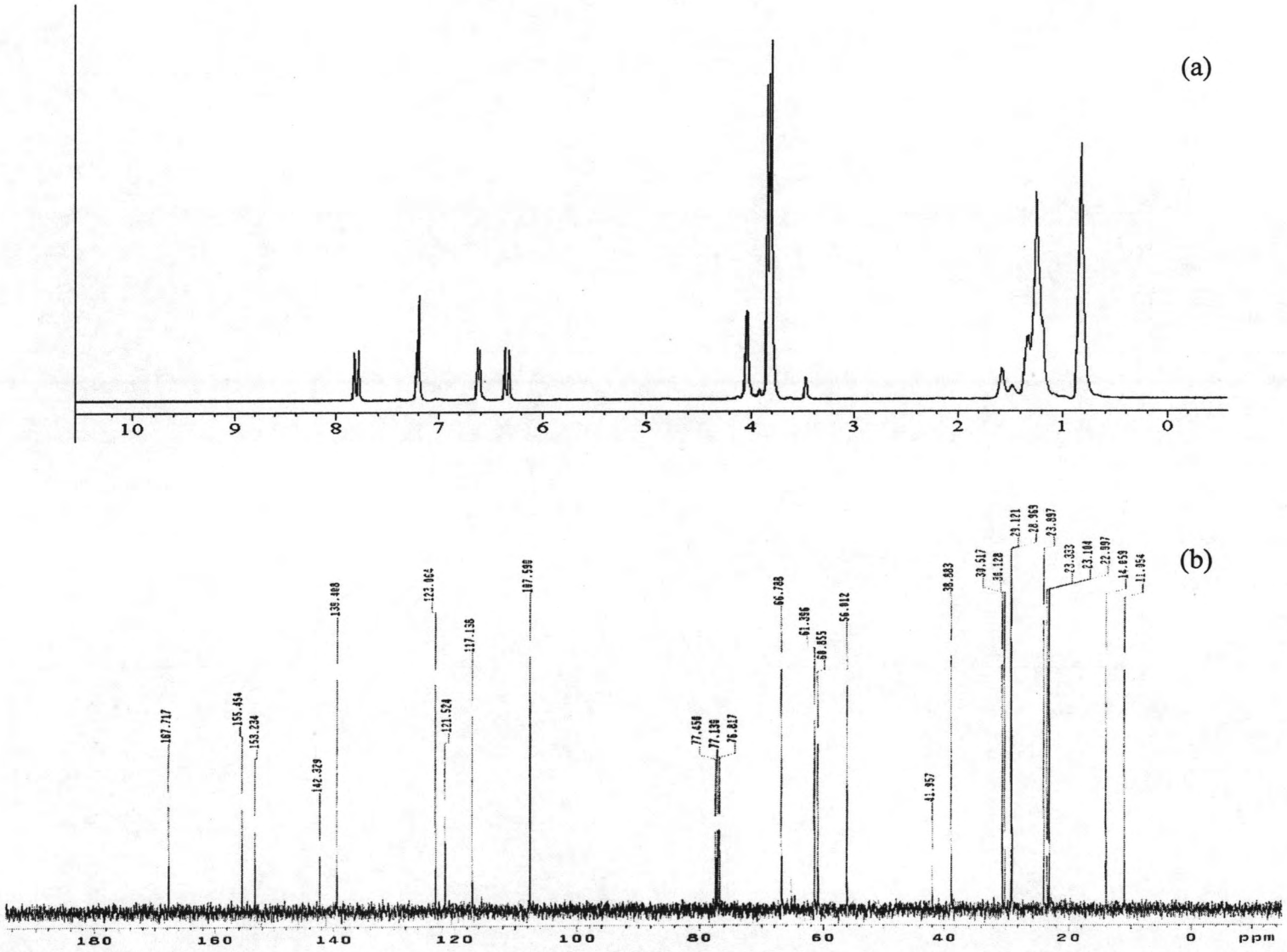

Figure A31 ^{1}H (a) and ^{13}C NMR spectrum (b) of 2-ethylhexyl-*trans*-2,3,4-trimethoxycinnamate (*trans*-**8E**) in $CDCl_3$.

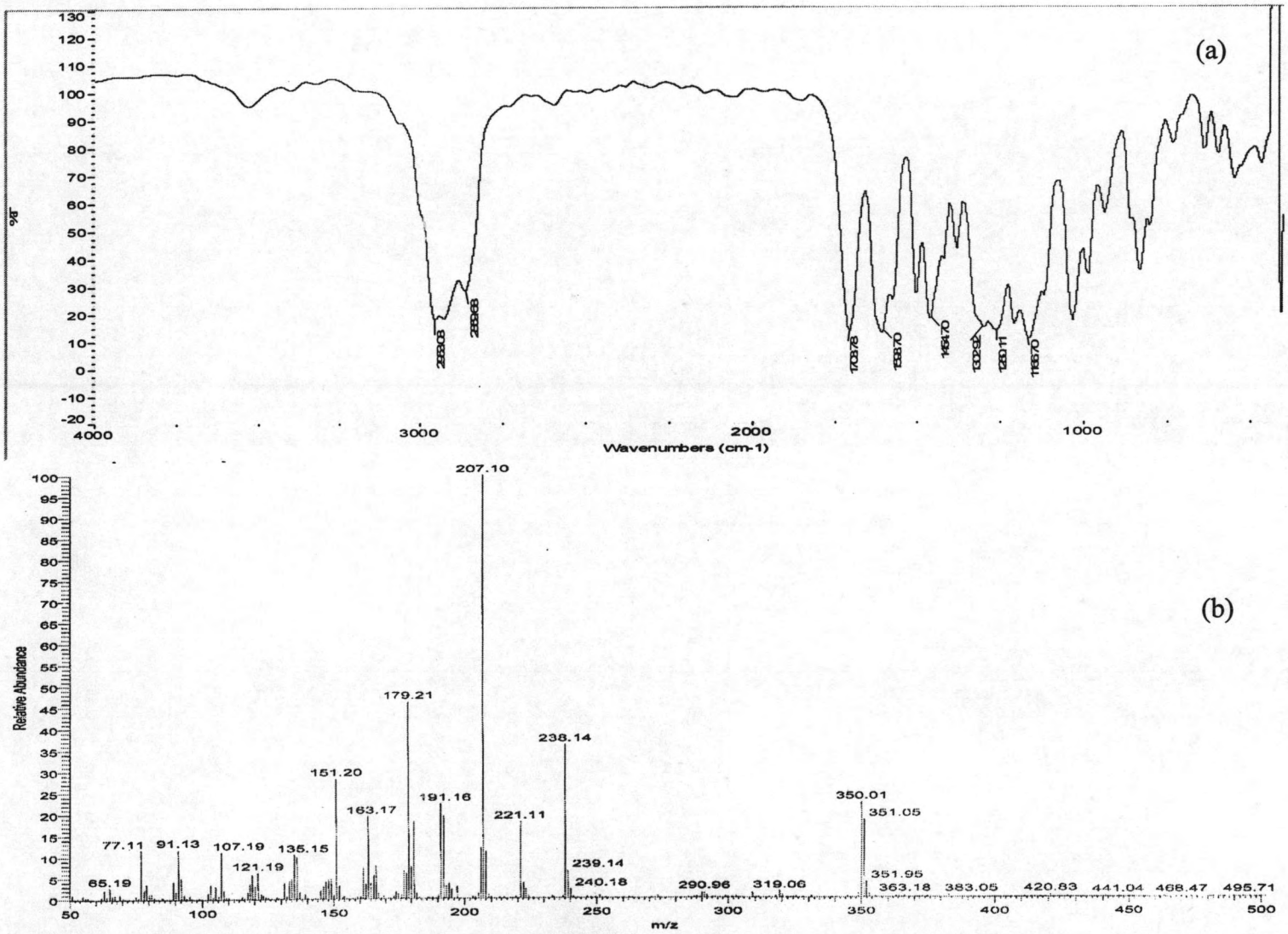

Figure A32 IR (a) and MS spectrum (b) of 2-ethylhexyl-*trans*-2,3,4-trimethoxycinnamate (*trans*-**8E**).

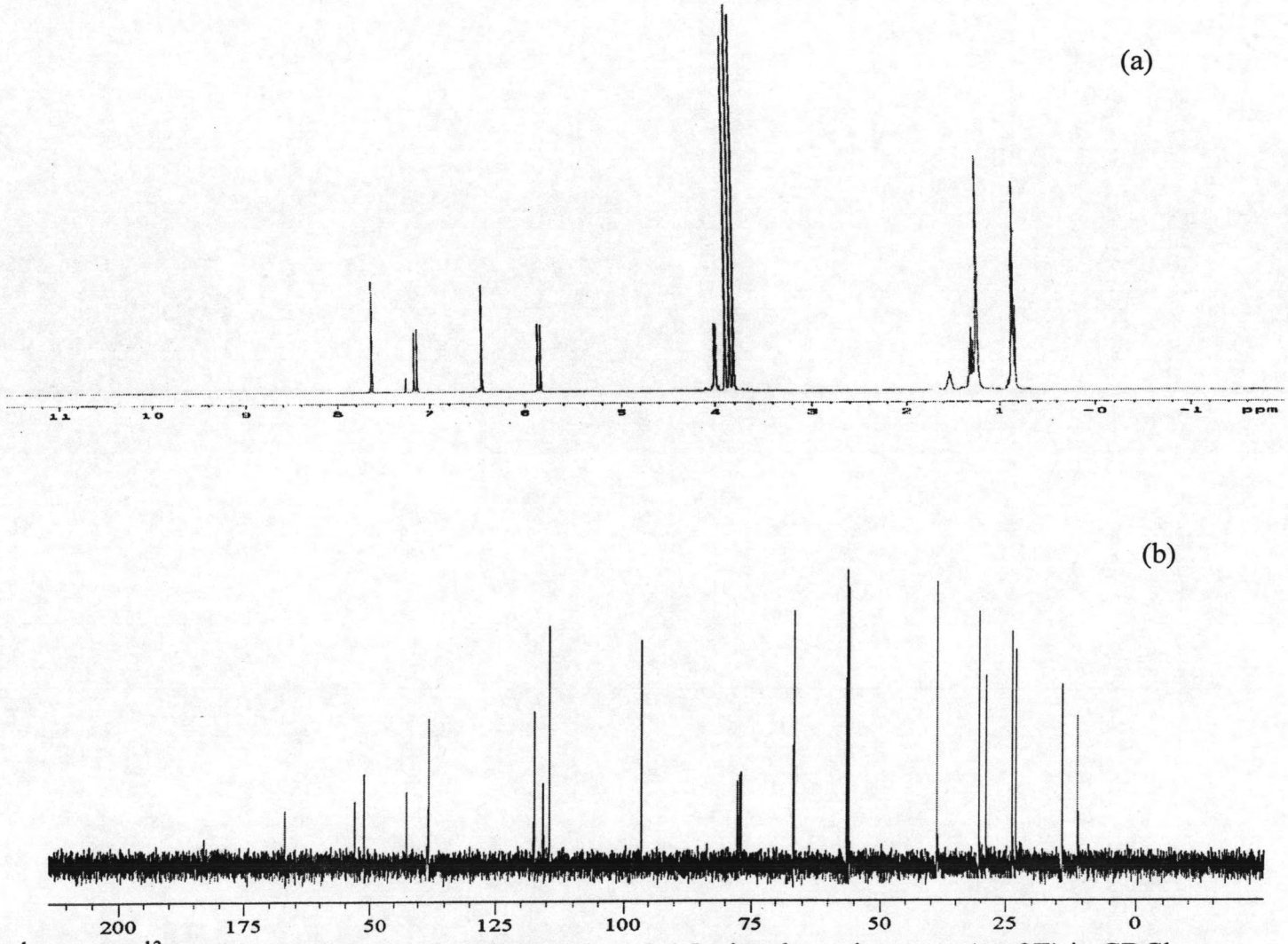

Figure A33 ^{1}H (a) and ^{13}C NMR spectrum (b) of 2-ethylhexyl-*cis*-2,4,5-trimethoxycinnamate (*cis*-**9E**) in $CDCl_3$.

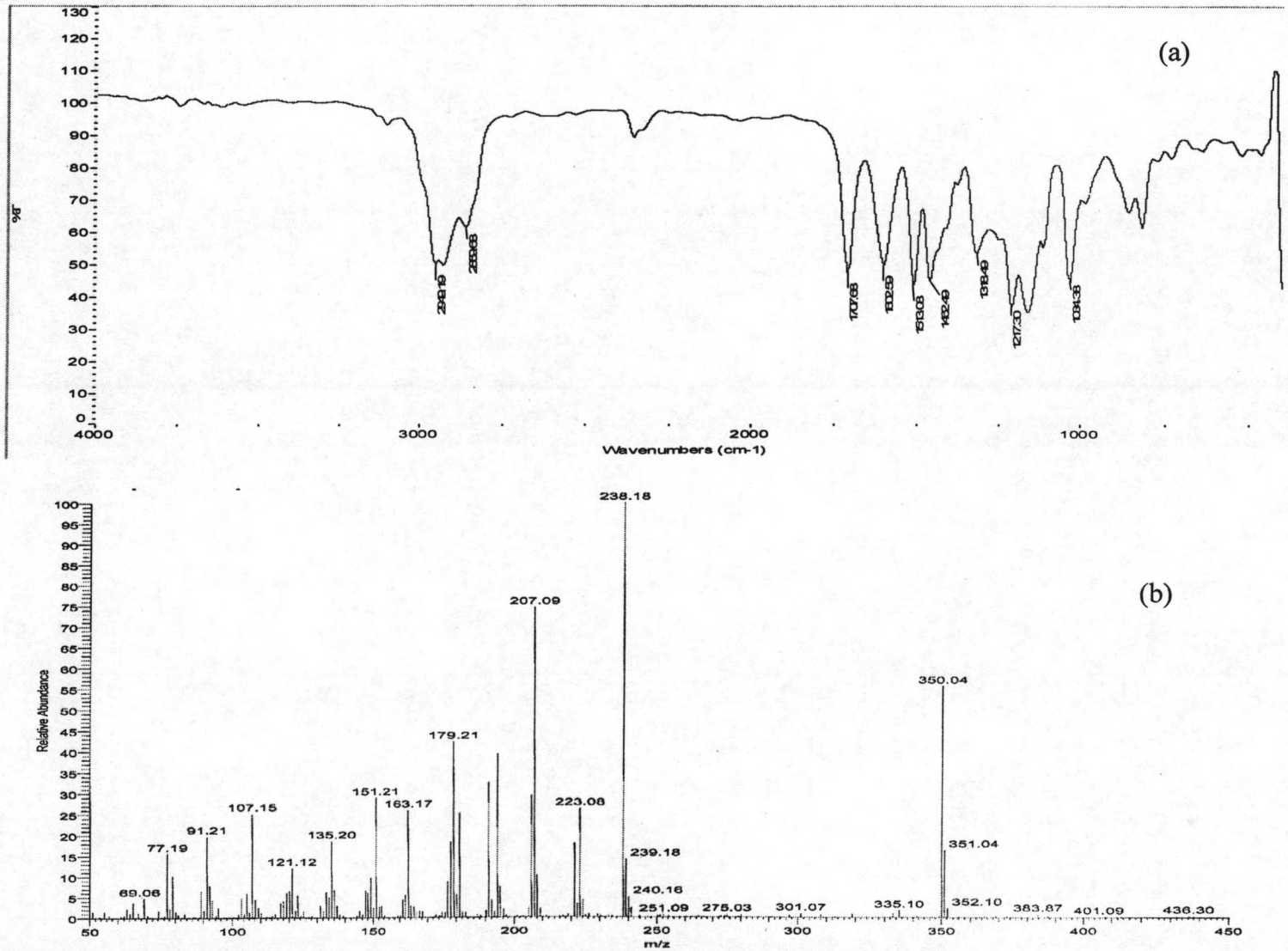

Figure A34 IR (a) and MS spectrum (b) of 2-ethylhexyl-*cis*-2,4,5-trimethoxycinnamate (*cis*-**9E**).

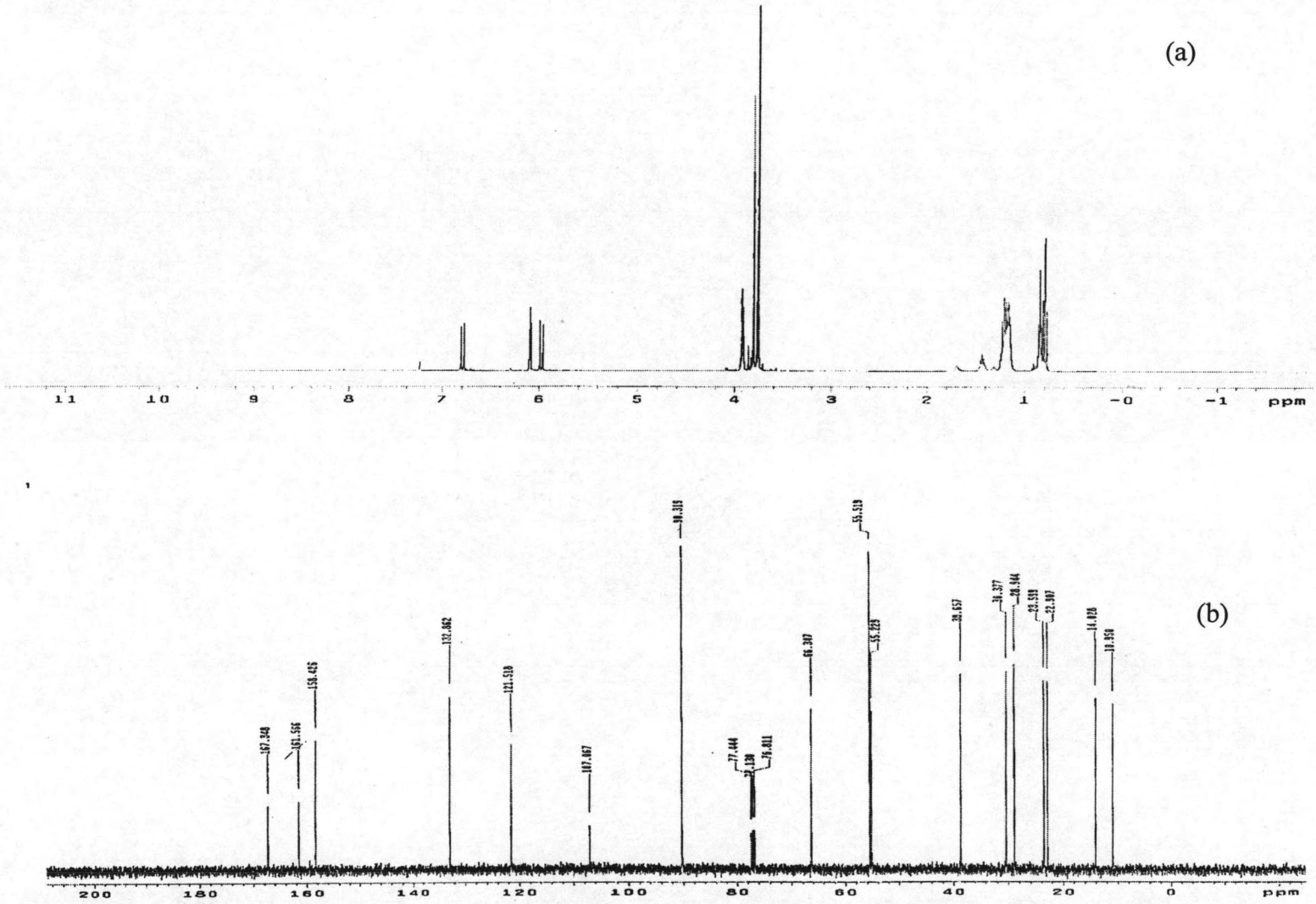

Figure A35 ^{1}H (a) and ^{13}C NMR spectrum (b) of 2-ethylhexyl-*cis*-2,4,6-trimethoxycinnamate (*cis*-**10E**) in $CDCl_3$.

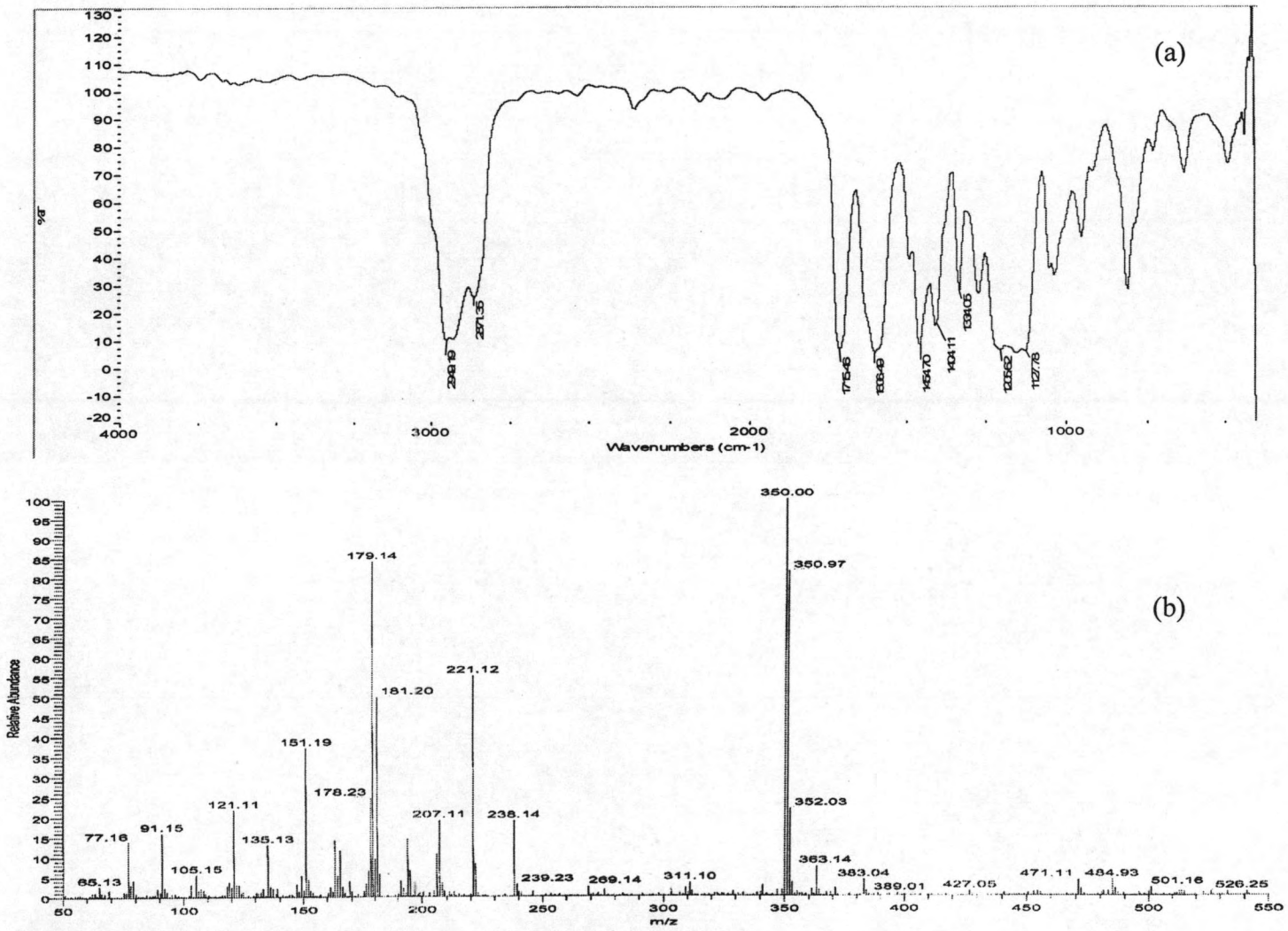

Figure A36 IR (a) and MS spectrum (b) of 2-ethylhexyl-*cis*-2,4,6-trimethoxycinnamate (*cis*-**10E**).

Appendix B

1. Solvent effect to absorption and emission maxima of five selected cinnamates.

The absorption and emission spectra of five *trans* and *cis*-cinnamates were carried out in methanol, dimethylsulfoxide (DMSO), acetonitrile, tetrahydrofuran (THF), dichloromethane and hexane. The absorption and emission maxima of each cinnamate in various solvents were reported in Table B1.

Table B1 Absorption, emission maxima wavelength of cinnamates in various solvents

Cpds	Abs. λ_{max}, Em.λ_{max} (nm)					
	MeOH	**DMSO**	**Acetonitrile**	**THF**	**DCM**	**Hexane**
trans-**1E**	323 (276), 410	327 (278), 400	323 (276), 393	323 (274), 378	319 (276), 386	320 (272), 359
cis-**1E**	313 (271), 409	311 (273), 395	312 (272), 397	313 (272), 378	309 (275), 382	311 (275), 361
trans-**2E**	314 (278), 409	316 (281), 398	312 (276), 385	311 (278), 368	312 (278), 380	312 (273), 350
cis-**2E**	313 (274), 410	313 (274), 396	311 (276), 410	313 (274), 370	308 (273), 378	308 (275), 351
trans-**3E**	310, 462	312, 349	308, 375	309, 372	306, 374	290, 351
cis-**3E**	303, 468	308, 371	300, 384	309, 372	296, 378	305, 354
trans-**9E**	349, 461	357, 442	349, 438	350, 417	350, 432	349, 398
cis-**9E**	345, 461	347, 444	342, 441	350, 416	350, 431	345, 397
trans-**10E**	320, 463	324, 367	317, 396	319, 367	317, 388	304, 358
cis-**10E**	305, 458	307, 369	303, 394	302, 368	300, 381	298, 340

2. Calculation of the radiative rate constants (k_f)

The radiative rate constants of all cinnamates in methanol and hexane have been calculated using the Strickler-Berg relationship as equation below:

$$k_f = 2.88 \times 10^{-9}\, n^2\, \tilde{\nu}^2 \int \varepsilon(\tilde{\nu})\, d\tilde{\nu}$$

where $\varepsilon(\nu)$ is the molar absorption spectrum on a wavenumber (cm^{-1}) scale, n is the refractive index of the solvent, and ν is the mean transition energy between absorption and emission spectra.

The Gaussian fit were shown below and the integral of molar absorption spectrum on a wavenumber scale in methanol and hexane form Gaussian fit reported in Table 1 and 2, respectively.

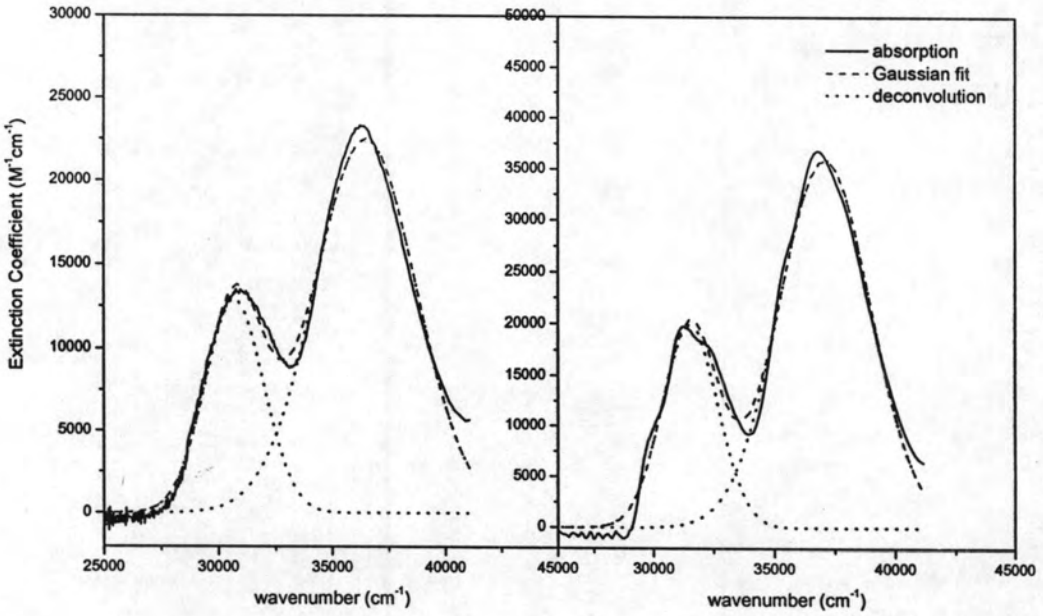

Figure B1 Gaussian fit of *trans*-**1E** in methanol (left) and hexane (right).

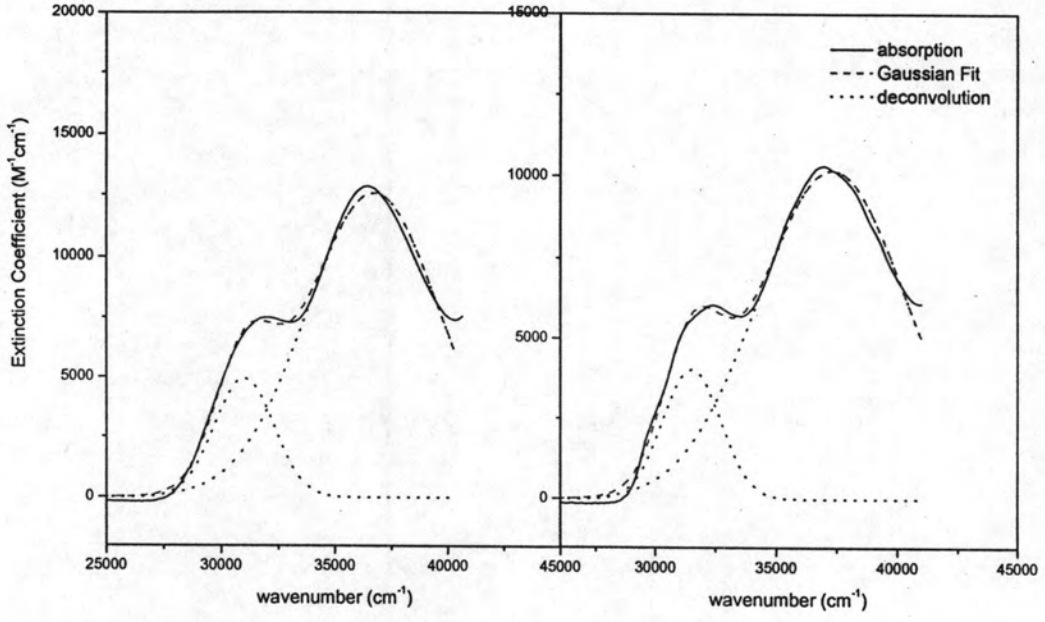

Figure B2 Gaussian fit of *cis*-**1E** in methanol (left) and hexane (right).

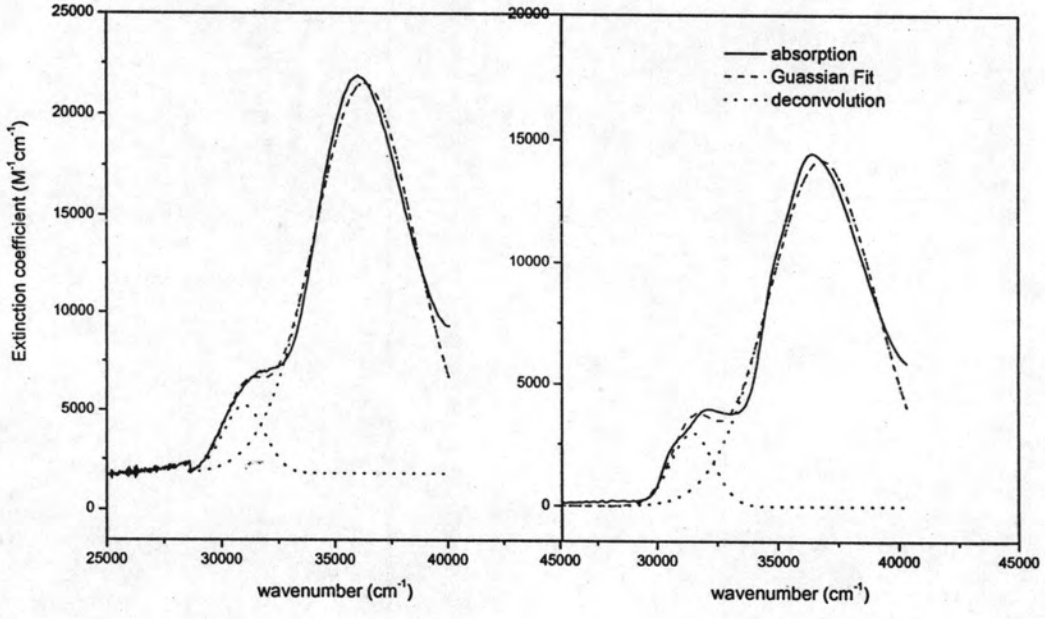

Figure B3 Gaussian fit of *trans*-**2E** in methanol (left) and hexane (right).

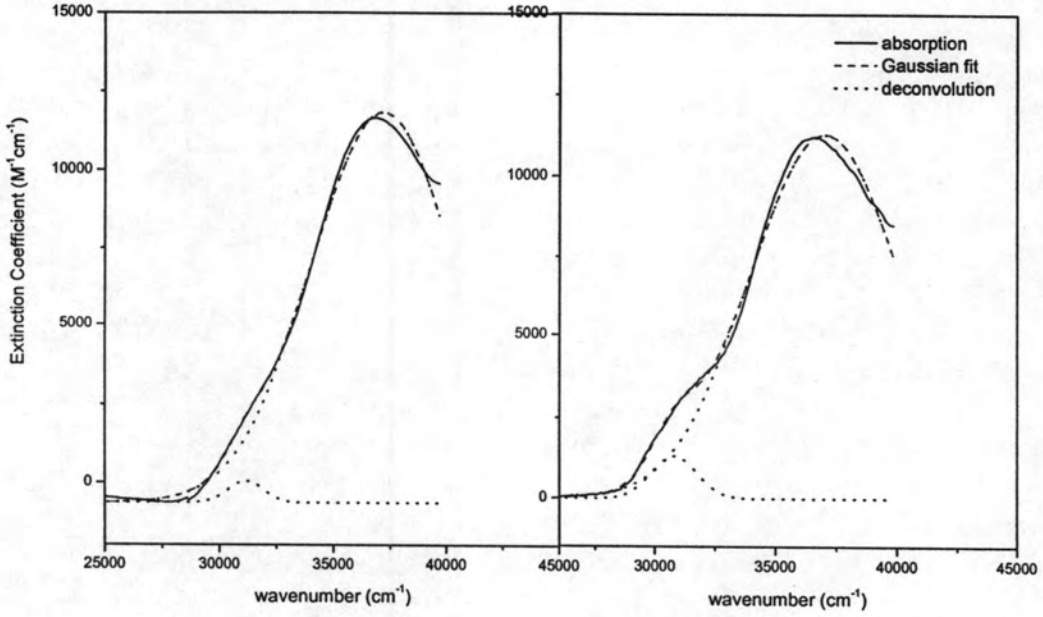

Figure B4 Gaussian fit of *cis*-**2E** in methanol (left) and hexane (right).

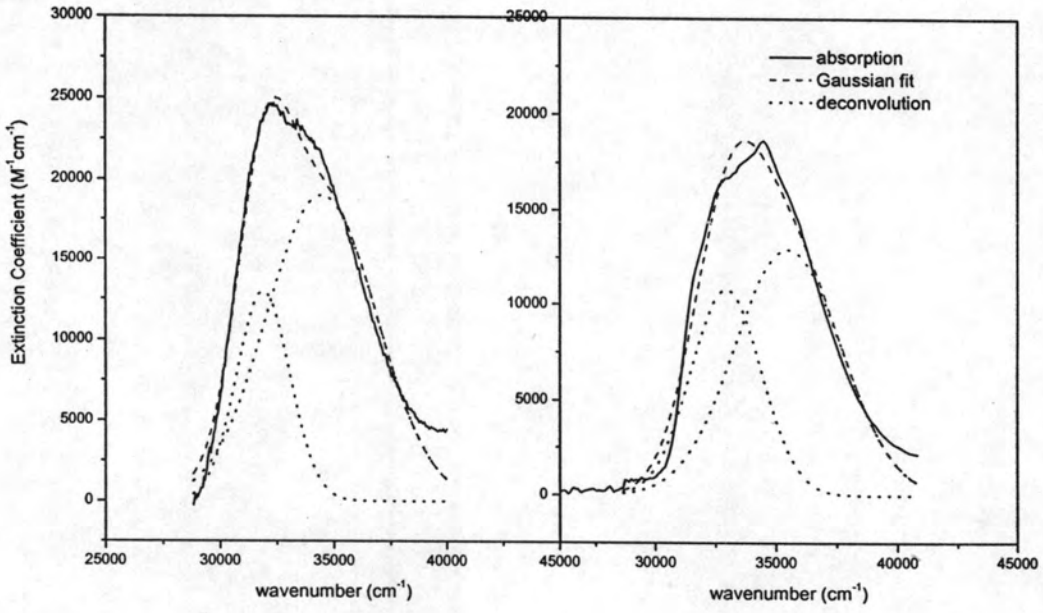

Figure B5 Gaussian fit of *trans*-**3E** (left) in methanol and hexane (right).

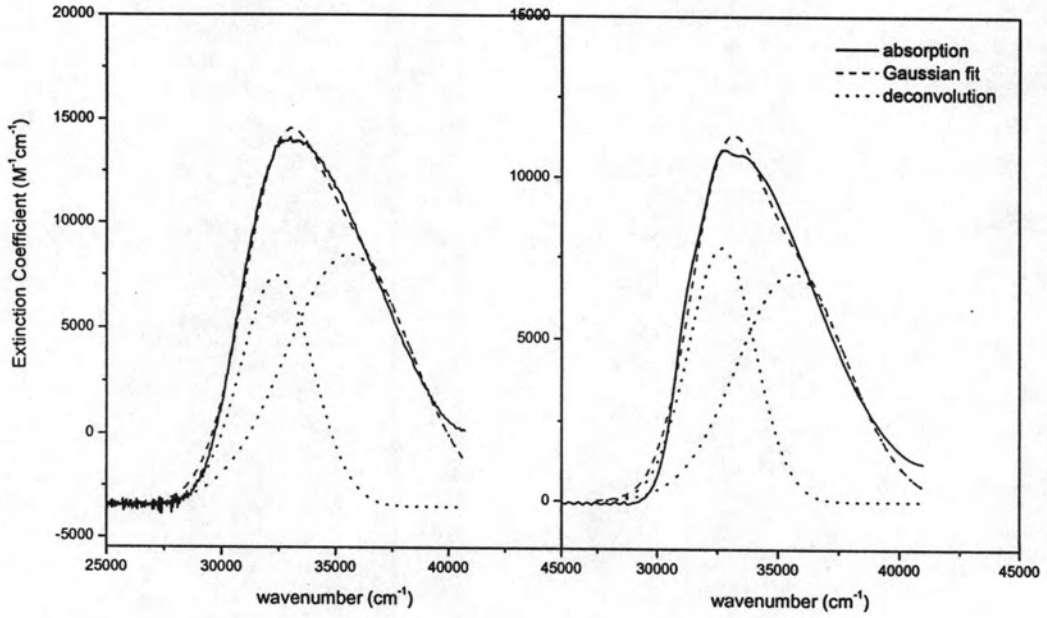

Figure B6 Gaussian fit of *cis*-**3E** in methanol (left) and hexane (right).

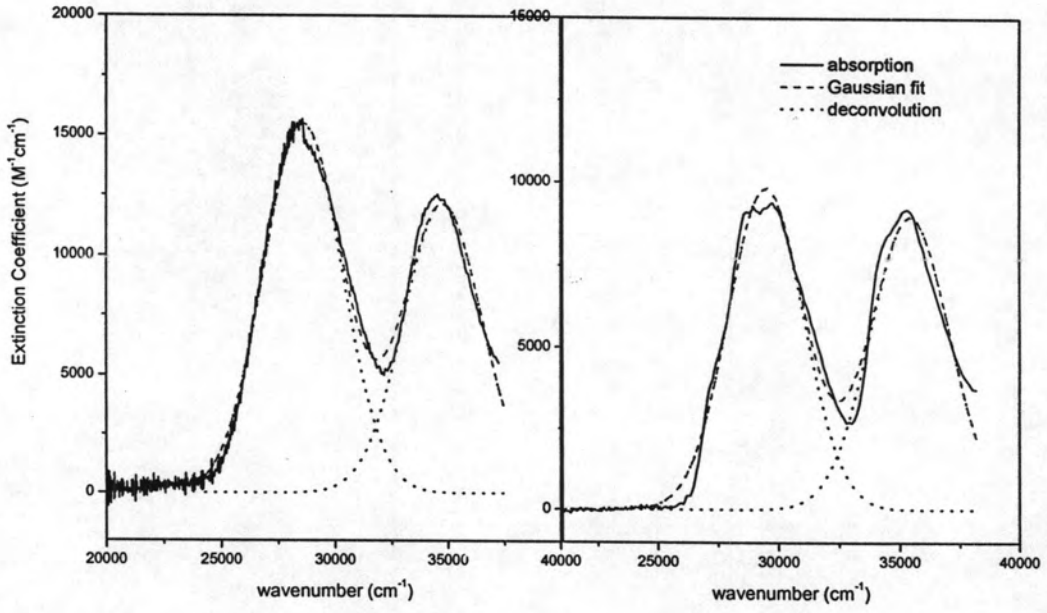

Figure B7 Gaussian fit of *trans*-**9E** in methanol (left) and hexane (right).

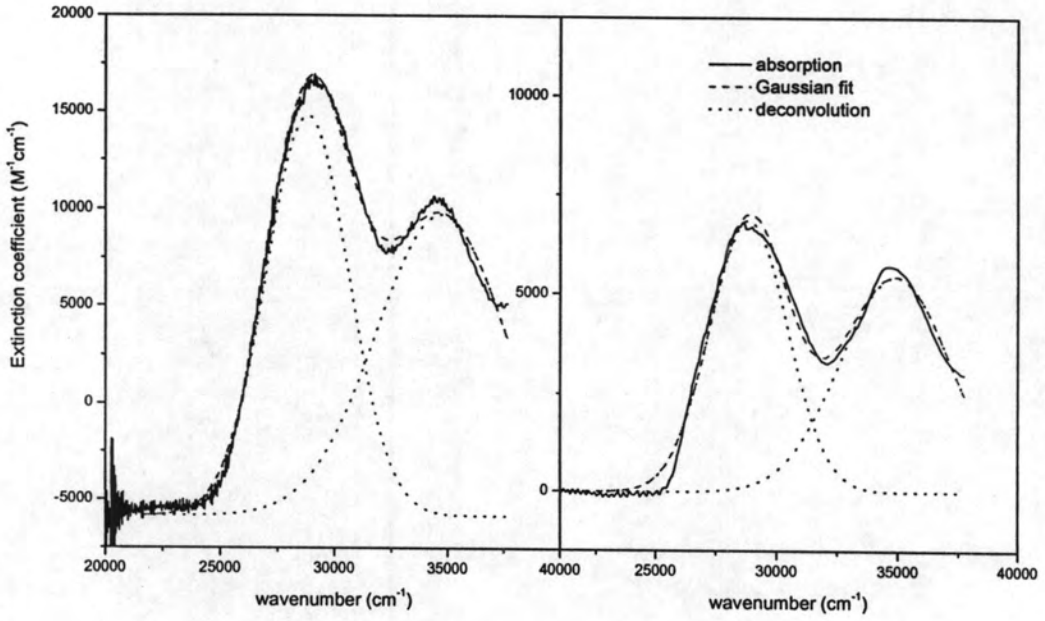

Figure B8 Gaussian fit of *cis*-**9E** in methanol (left) and hexane (right).

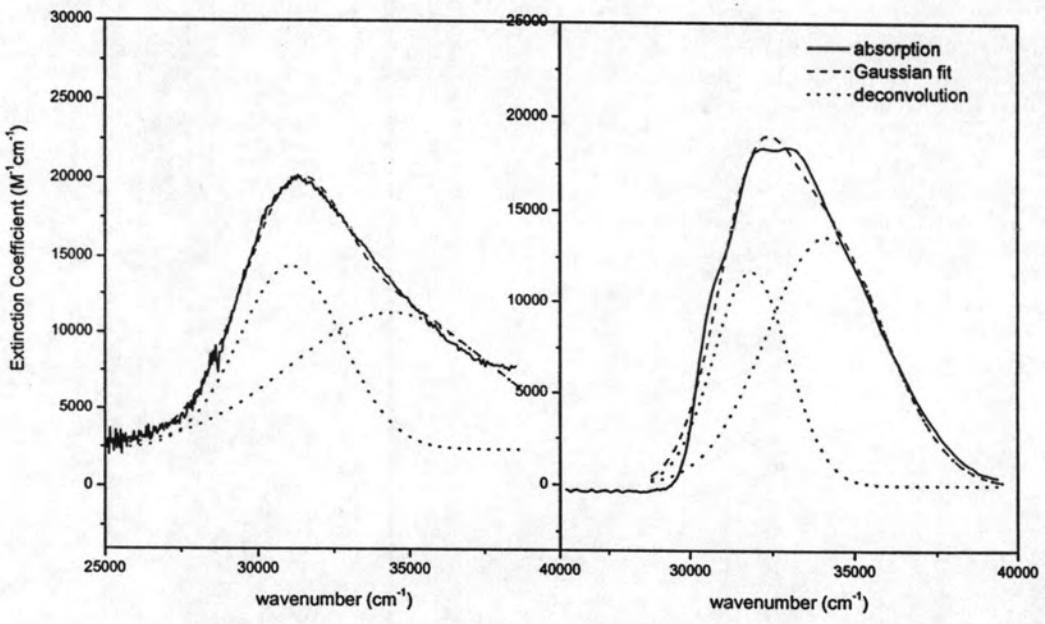

Figure B9 Gaussian fit of *trans*-**10E** in methanol and hexane.

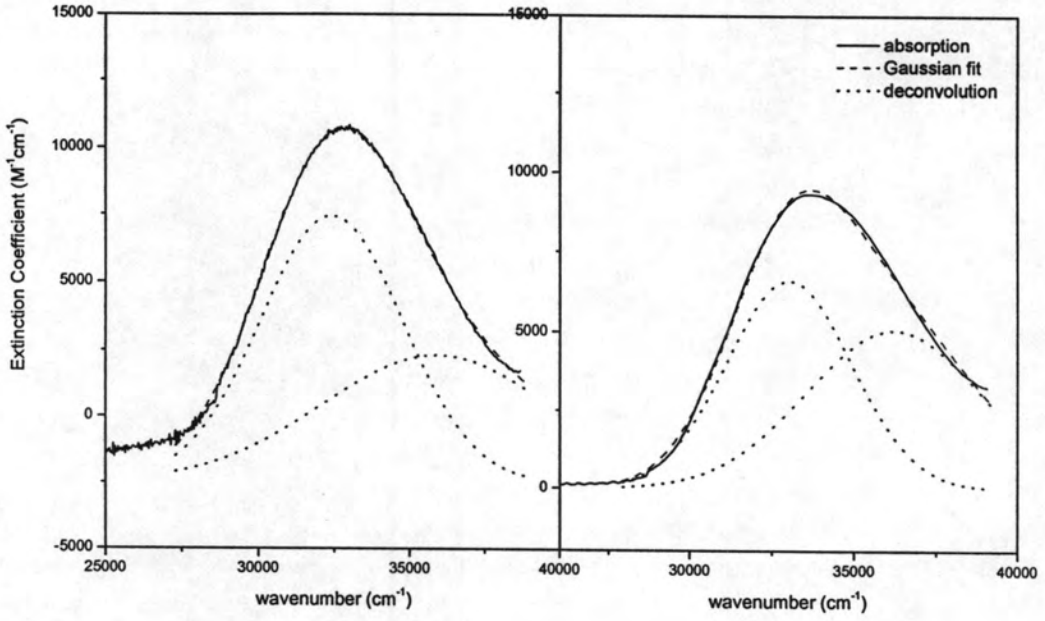

Figure B10 Gaussian fit of *cis*-**10E** in methanol and hexane.

Table B2 Integrate peak area from Gaussian fit of cinnamates in methanol.

cpds	Peak area (x 10^7)		R^2
	Peak area 1	Peak area 2	
t-**1E**	5.78	17.05	0.990
c-**1E**	1.60	9.40	0.997
t-**2E**	0.76	11.10	0.990
c-**2E**	0.14	9.99	0.995
t-**3E**	3.82	11.46	0.983
c-**3E**	4.40	8.41	0.997
t-**9E**	6.73	5.32	0.986
c-**9E**	9.40	11.29	0.997
t-**10E**	5.05	3.31	0.992
c-**10E**	5.89	4.59	0.999

Table B3 Integrate peak area from Gaussian fit of cinnamates in hexane.

cpds	Peak area ($\times 10^7$)		R^2
	Peak area 1	Peak area 2	
t-**1E**	4.17	12.64	0.990
c-**1E**	1.21	7.86	0.996
t-**2E**	0.65	7.86	0.992
c-**2E**	0.31	8.80	0.997
t-**3E**	3.95	7.09	0.982
c-**3E**	2.72	4.04	0.989
t-**9E**	3.86	3.71	0.986
c-**9E**	2.76	3.11	0.992
t-**10E**	3.31	6.19	0.990
c-**10E**	3.17	3.40	0.998

3. Potential surface energy calculation

Quantum mechanical calculations were performed by the semi-empircal methods PM3 (ground state optimization) and ZINDO/S (excited state energies and transition moments) as implemented in the Hyperchem 5.1 program. The potential surface energy of each compound was shown in Table B3-B7. The plot energies of each compound are related to the energy at tosion angle 180 of S_0 state.

Table B4 Potential energy surface of **1E**.

Torsion angle	ΔH_f (kcal mol^{-1})			
	S_0	S_1	S_2	S_3
0	-115.13	-23.2631	-15.137	-2.47835
10	-114.57	-23.6118	-15.026	-4.06849
20	-113.23	-23.4115	-14.2886	-5.29325
30	-111.16	-22.3732	-13.0905	-6.00908
40	-108.33	-20.6618	-11.5907	-6.1689
50	-104.7	-18.0255	-10.092	-5.33924
60	-102.91	-21.0038	-14.7744	-8.90527
70	-99.32	-24.8757	-13.2377	-8.06573
80	-97.82	-32.0593	-10.3983	-6.3907
90	-96.4	-76.4963	-41.3089	4.19088
100	-97.15	-32.1249	-6.31021	-5.57139
110	-97.46	-22.056	-9.64643	-6.17952
120	-100.5	-17.4546	-12.4187	-6.486
130	-102.49	-14.7411	-9.72321	-4.33302
140	-106.61	-19.3297	-11.9801	-6.84024
150	-109.87	-22.7599	-14.0416	-8.33995
160	-112.15	-25.336	-15.6588	-9.22788
170	-113.5	-27.4254	-16.7934	-9.91434
180	-113.91	-28.4425	-17.2132	-10.253

Table B5 Potential energy surface of **2E**.

Torsion angle	ΔH_f (kcal mol^{-1})			
	S_0	S_1	S_2	S_3
0	-116.59	-24.7556	-15.5692	1.2461
10	-116.05	-24.9991	-15.5651	-0.48978
20	-114.71	-24.6398	-14.8322	-2.32837
30	-112.59	-23.4823	-13.3912	-3.62517
40	-109.68	-21.826	-11.5062	-4.99479
50	-105.9	-18.917	-9.1967	-5.34095
60	-102.54	-15.5703	-5.86612	-3.06174
70	-100.55	-22.7544	-12.9462	-10.238
80	-97.35	-28.7764	-10.7673	-6.36861
90	-95.8	-71.1875	-27.1127	-8.97811
100	-97.63	-27.2231	-7.26094	-6.09535
110	-97.63	-22.7544	-12.9462	-10.238
120	-104.09	-18.9938	-15.5095	-11.5813
130	-106.19	-17.7956	-10.4482	-8.91109
140	-110.43	-22.5193	-13.8834	-9.94161
150	-113.73	-26.5561	-16.7019	-10.7152
160	-116.07	-29.7095	-18.7613	-11.4422
170	-117.45	-31.9365	-20.0253	-12.0938
180	-117.92	-32.5622	-20.4388	-12.2797

Table B6 Potential energy surface of **3E**.

Torsion angle	ΔH_f (kcal mol^{-1})			
	S_0	S_1	S_2	S_3
0	-117.74	-26.1409	-17.6385	-6.66341
10	-117.05	-24.6936	-17.1687	-6.48014
20	-115.55	-24.6871	-15.8602	-9.72598
30	-113.54	-24.271	-14.3068	-11.6954
40	-110.72	-22.9819	-12.7547	-11.8436
50	-107.22	-20.8647	-19.0572	-8.9686
60	-106.11	-24.3092	-17.524	-10.7671
70	-102.71	-28.0364	-16.4251	-10.1084
80	-99.74	-34.1647	-14.2341	-7.34483
90	-96.55	-73.8336	-31.3841	8.33485
100	-98.37	-30.3622	-7.64547	-4.67324
110	-101.27	-25.8719	-12.9684	-8.19831
120	-104.76	-21.9287	-16.2069	-9.77495
130	-106.89	-17.9099	-14.5992	-9.08547
140	-111.12	-22.4186	-15.7581	-12.7233
150	-114.39	-26.5171	-16.9387	-15.5444
160	-116.69	-29.8945	-18.1305	-17.5531
170	-118.06	-32.0786	-19.0021	-18.7717
180	-118.5	-32.7249	-19.2806	-19.1151

Table B7 Potential energy surface of **9E**.

Torsion angle	ΔH_f (kcal mol^{-1})			
	S_0	S_1	S_2	S_3
0	-187.22	-95.3059	-93.603	-80.5712
10	-186.97	-94.6434	-93.4142	-80.1659
20	-184.57	-92.1898	-91.2249	-78.6284
30	-181.69	-89.5805	-88.5425	-76.9588
40	-179.37	-87.8968	-86.6694	-76.7765
50	-174.54	-84.4215	-82.6849	-75.3825
60	-172.4	-92.0449	-86.9555	-81.9681
70	-169.6	-95.7897	-85.4527	-81.9157
80	-167.18	-166.044	-103.201	-83.2426
90	-165.77	-143.042	-108.776	-67.4781
100	-167.26	-159.66	-103.71	-78.9175
110	-169.97	-100.586	-86.3443	-82.8466
120	-173.36	-95.4457	-88.1522	-83.3606
130	-175.2	-89.0373	-87.3541	-80.4321
140	-179.64	-92.8682	-90.5184	-82.9988
150	-183.12	-95.861	-92.8707	-84.591
160	-185.52	-98.5106	-94.7436	-85.9066
170	-186.93	-100.337	-95.9457	-86.825
180	-187.34	-101.211	-96.3875	-87.284

Table B7 Potential energy surface of **10E**.

Torsion angle	ΔH_f (kcal mol^{-1})			
	S_0	S_1	S_2	S_3
0	-187.9	-99.7155	-91.8495	-82.6058
10	-187.52	-101.021	-91.4663	-84.4384
20	-185.99	-99.5199	-90.4273	-85.0298
30	-182.19	-95.7643	-87.7663	-84.3754
40	-179.65	-93.0699	-84.8507	-82.7993
50	-176.46	-90.8159	-84.1722	-82.8767
60	-172.97	-92.2634	-84.1474	-82.1619
70	-169.82	-97.9354	-82.7735	-81.9336
90	-167.15	-147.779	-104.906	-71.1801
110	-170.74	-97.3295	-83.6458	-82.5609
120	-174.45	-94.2346	-86.0611	-85.4283
130	-176.12	-87.8029	-86.3707	-84.555
140	-180.7	-92.1222	-88.3973	-87.4554
150	-183.83	-96.1161	-90.7492	-88.7154
160	-186.13	-98.8737	-92.6446	-89.4888
170	-187.48	-100.792	-93.8017	-89.9656
180	-187.92	-101.596	-94.2509	-90.3457

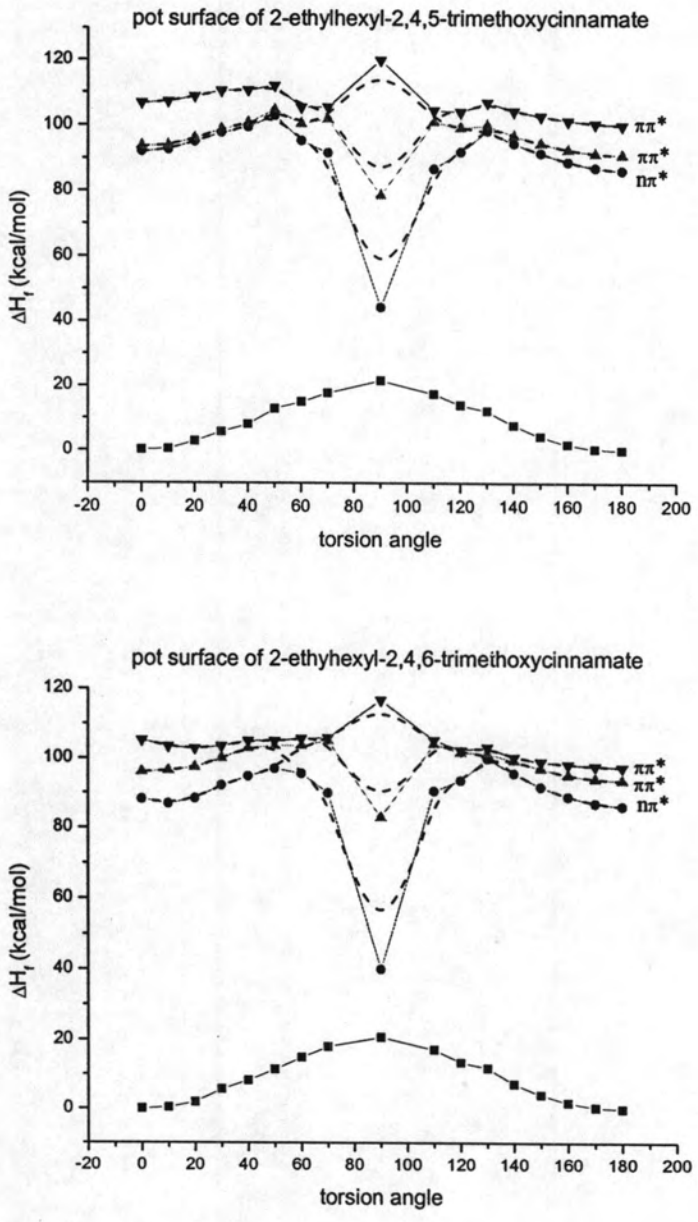

Figure B11. Calculated potential energy surfaces for **9E** and **10E** (PM3 + INDO/S-CI,).The approximate adiabatic potential surfaces are shown with dashed lines.

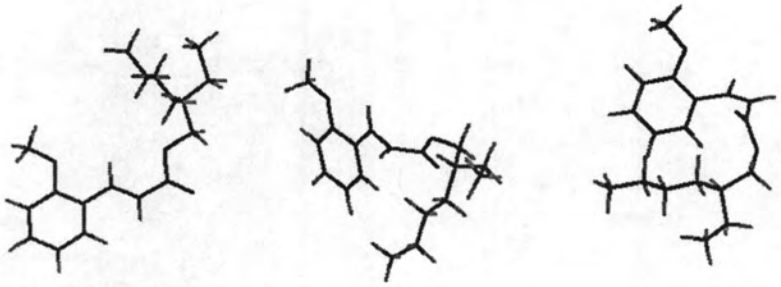

Figure B12 Optimization structures of 2-ethylhexyl-2-methoxycinnamate (**1E**); torsion angle= 180° (left), 90° (middle) and 0° (right); green = carbon, gray = hydrogen and red = oxygen

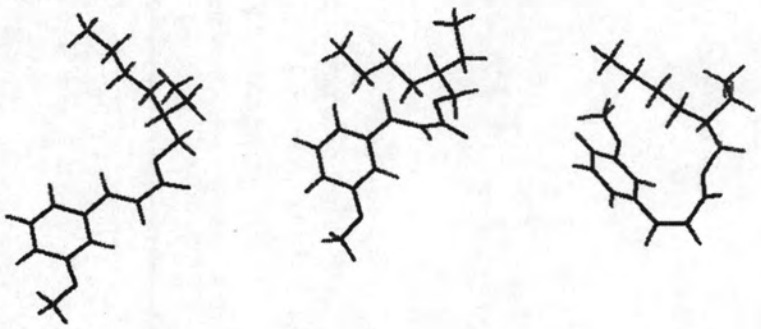

Figure B13 Optimization structures of 2-ethylhexyl-3-methoxycinnamate (**2E**); torsion angle= 180° (left), 90° (middle) and 0° (right); green = carbon, gray = hydrogen and red = oxygen

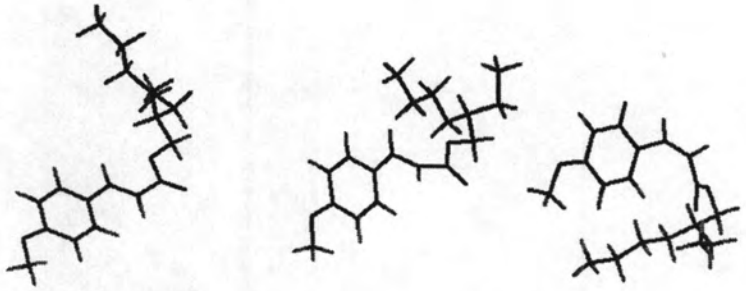

Figure B14 Optimization structures of 2-ethylhexyl-4-methoxycinnamate (**3E**); torsion angle= 180° (left), 90° (middle) and 0° (right); green = carbon, gray = hydrogen and red = oxygen.

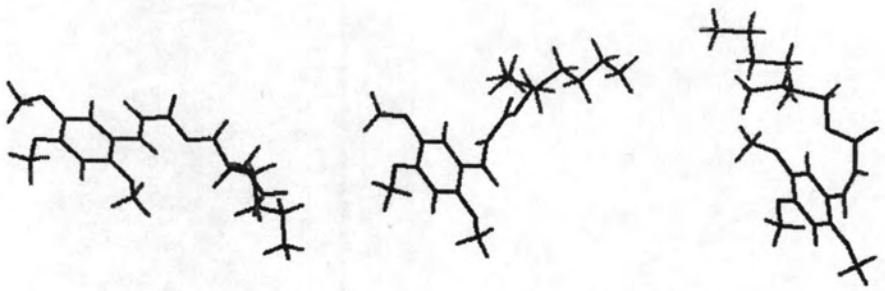

Figure B15 Optimization structures of 2-ethylhexyl-2,4,5-trimethoxycinnamate (**9E**); torsion angle= 180° (left), 90° (middle) and 0° (right); green = carbon, gray = hydrogen and red = oxygen

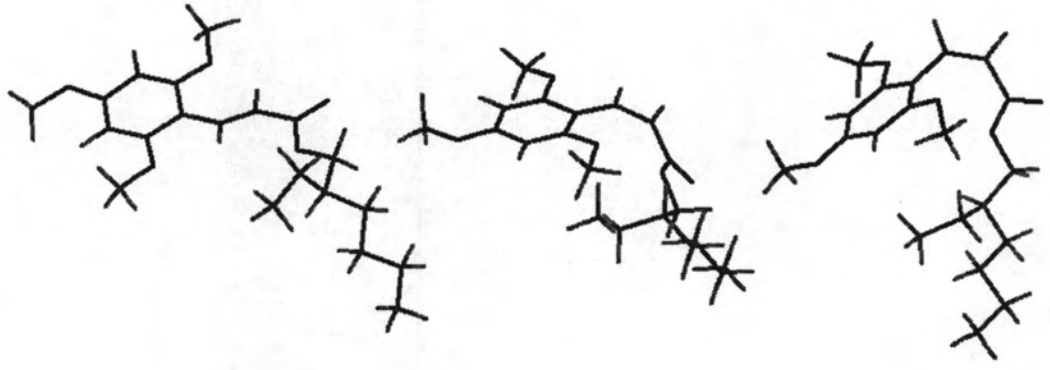

Figure B16 Optimization structures of 2-ethylhexyl-2,4,6-trimethoxycinnamate **(10E)**; torsion angle= 180° (left), 90° (middle) and 0° (right); green = carbon, gray = hydrogen and red = oxygen

VITA

I was born on August 19th, 1980 in Bangkok, Thailand. I got a Bachelor and Master Degree of Science in Chemistry from Chulalongkorn University in 2001 and 2003, respectively. Since then, I have been a Ph.D. student studying in Organic Chemistry at Chulalongkorn Univeristy. During my studies towards the Ph.D., I was granted by Royal Golden Jubilee Ph.D. program, Thailand Research Fund.

My address is 444/1 Phahonyothin 24 Phahonyothin Road Chatuchak Bangkok 10900, Tel. 0-2513-5093, 081-735-5093.